1999

Identification and characterization of a unique DNA-binding protein in Borrelia burgdorferi

Scott W. Knight
The University of Montana

INFORMATION TO USERS

This manuscript has been reproduced from the microfilm master. UMI films the text directly from the original or copy submitted. Thus, some thesis and dissertation copies are in typewriter face, while others may be from any type of computer printer.

The quality of this reproduction is dependent upon the quality of the copy submitted. Broken or indistinct print, colored or poor quality illustrations and photographs, print bleedthrough, substandard margins, and improper alignment can adversely affect reproduction.

In the unlikely event that the author did not send UMI a complete manuscript and there are missing pages, these will be noted. Also, if unauthorized copyright material had to be removed, a note will indicate the deletion.

Oversize materials (e.g., maps, drawings, charts) are reproduced by sectioning the original, beginning at the upper left-hand corner and continuing from left to right in equal sections with small overlaps. Each original is also photographed in one exposure and is included in reduced form at the back of the book.

Photographs included in the original manuscript have been reproduced xerographically in this copy. Higher quality 6" x 9" black and white photographic prints are available for any photographs or illustrations appearing in this copy for an additional charge. Contact UMI directly to order.

UMI®

Bell & Howell Information and Learning
300 North Zeeb Road, Ann Arbor, MI 48106-1346 USA
800-521-0600

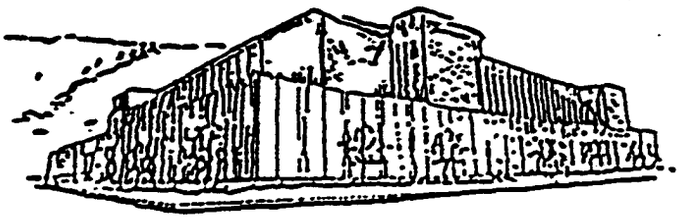

Maureen and Mike
MANSFIELD LIBRARY

The University of **MONTANA**

Identification and Characterization of a Unique DNA-Binding Protein in *Borrelia burgdorferi*

Scott W. Knight

B. S. Linfield College, McMinnville, Oregon 1994

Presented in partial fulfillment of the requirements for the degree of

Doctor of Philosophy

The University of Montana

1999

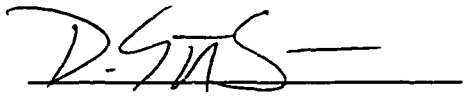

Chairman, Board of Examiners

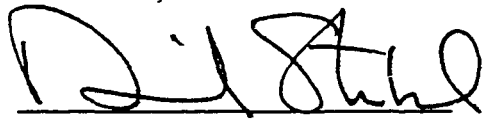

Dean, Graduate School

6-14-99

Date

Knight, Scott W., Ph.D., June 1999

Biochemistry and Microbiology
Molecular Biology emphasis

Identification and Characterization of a Unique DNA-Binding Protein in *Borrelia burgdorferi*

Director: Dr. D. Scott Samuels DSS

We have identified a 35-kDa HU-like protein in the Lyme disease spirochete *Borrelia burgdorferi*, a bacterium with a predominantly linear genome. The 35-kDa protein is translated from an abundant transcript initiated within the gene encoding the A subunit of DNA gyrase. Translation of the 35-kDa protein starts at residue 499 of GyrA and proceeds in the identical reading frame as full-length GyrA, resulting in an N-terminal-truncated protein. The 35-kDa GyrA C-terminal domain, though lacking sequence similarity, substitutes for HU in the formation of the Type 1 complex in Mu transposition and complements an HU deficient strain of *Escherichia coli*. This is the first example of constitutive expression of two gene products in the same open reading frame from a single gene in a prokaryotic cellular system.

The GyrA C-terminal domain binds DNA with an apparent dissociation constant of approximately 1×10^{-8} M. Binding of the protein induces DNA conformational changes by either bending or wrapping the helix. These induced conformational changes are similar to the interaction between the *E. coli* HU protein and DNA. Unlike HU, however, the GyrA C-terminal domain prefers binding linear substrates rather than prebent molecules. These findings indicate that the GyrA C-terminal domain may be involved in bending and compacting the predominantly linear genome of *B. burgdorferi*, or in DNA transactions requiring a distorted helix. To begin to understand the role of this unique protein in *B. burgdorferi*, we have genetically disrupted synthesis of the GyrA C-terminal domain and are beginning to examine the mutant spirochetes for a phenotype.

Acknowledgements

I would like to thank Scott Samuels for his support and mentoring during my tenure at the University of Montana. I am grateful to him for allowing me to join his laboratory, for his outstanding scientific ideas, and his tremendous editorial skills. My thanks to the members of my graduate committee, Mike Minnick, Walt Hill, Jack Nunberg, and Keith Parker, for their guidance and support. I thank my friends and co-workers, Christian Eggers, Betsy Kimmel, Janet Alverson, Corbin Schwanke, Kendal Galbraith, and the other members of the Samuels laboratory for their advice, technical assistance, and good times.

Special thanks to George Chaconas and Kit Tilly for suggesting experiments, providing technical advice, supplying critical reagents for completing this work, and for their helpful manuscript reviews. Others who have contributed to this work by providing reagents, advice, and assistance include: Tony Maxwell, Karl Drlica, Rich Marconi, Jason Carlyon, Chuck Sohaskey, Stuart Hill, Scott Manning, Joe Hinnebusch, and Bill Holben.

I thank my family, especially my Mom, Dad, and Grandparents for their love, encouragement, and support. Finally, I thank my wife, Tasha Knight, and dedicate this work to her. She has supported me through the highs and lows of my graduate career, edited hundreds of pages of text, and listened to many scientific ideas, both good and bad. Without her love, support, and sacrifices, the completion of this degree would not have been possible.

Table of Contents

List of Tables

List of Figures

Chapter 1

Introduction

1.1 Prokaryotic linear replicons.

Prokaryotic linear replicons were first discovered in *Streptomyces rochei* in 1979 (33). Linear DNA molecules have since been identified in a variety of prokaryotes including *Borrelia* species, *Rhodococcus fascians*, *Agrobacterium tumefaciens*, *Nocardia opaca*, and *Thiobacillus versutus* (36). Linear replicons require a different replication mechanism at the molecular ends, or telomeres, than at other positions, because of the enzymatic activities of DNA polymerases (101). These enzymes require a 3′-OH to initiate replication and to elongate a nascent daughter molecule (44). Under normal circumstances, the 3′-OH is provided by a short RNA primer that is later replaced by DNA (44). Replication of a linear molecule by this method results in a 3′-overhang at the telomere, and a 5′-unreplicated end, due to lagging strand synthesis. Eukaryotes have at least two different mechanisms to complete lagging-strand synthesis at the telomere: DNA synthesis from an RNA template via telomerase or recombination (5). Prokaryotes have also evolved at least two different mechanisms to complete telomeric replication, which differ significantly from those found in eukaryotes.

Prokaryotic linear replicons are classified into two categories based on the structure of the telomere (36). The first category, known as invertrons, is characterized by telomeres comprised of terminal proteins covalently attached to the 5′ end of each DNA strand (81). Invertrons solve the telomere lagging-strand replication problem by priming replication via a hydroxyl group provided by a serine, threonine, or tyrosine residue of the 5′ terminal protein (82). Linear plasmids in *Streptomyces* also contain a

centrally located origin of replication (16). Initiation at this origin results in bi-directional replication towards the telomeres, yielding replication intermediates with approximately 280-nucleotide 3′-overhangs (16). Lagging-strand synthesis is completed by protein-primed replication using the 3′-overhangs as a template (16).

The second category of prokaryotic linear replicons is characterized by the presence of hairpin loops at the telomeres (2, 36). The best example of this telomeric-structure is found in spirochetes in the genus *Borrelia*, which contain linear chromosomes and a number of linear and circular plasmids (26). The telomeric-structure of the *B. burgdorferi* linear chromosome and plasmids is similar, consisting of a palindromic AT-rich terminal hairpin loop and an approximately 20-bp inverted repeat (2, 26). The only other prokaryotic linear replicon identified to date containing hairpin loops at the telomeres is the prophage of coliphage N15 (36, 92).

B. burgdorferi, a causative agent of Lyme disease, is the best characterized species of *Borrelia*, and understanding the molecular biology of this organism is aided by the availability of a completely sequenced genome (26). With a linear chromosome and up to 17 circular and linear plasmids, the *B. burgdorferi* genome may be the most complex of those found in the prokaryotes (26, 80). *B. burgdorferi* strain B31, a commonly used laboratory strain, contains several linear plasmids, including a 56-kb plasmid, a 54-kb plasmid, four 28-kb plasmids, a 38-kb plasmid, a 25-kb plasmid, and a 17-kb plasmid (26). Circular plasmids include at least five 32-kb plasmids, a 26-kb plasmid, and a 9-kb plasmid (26). Some of these plasmids share regions of homologous sequence, further adding to the complexity of the genome (1, 14, 105). Encoded on the plasmids are genes for major outer membrane proteins and important biosynthetic genes,

including *guaA* and *guaB* (54). Based on the linear structure of the majority of the plasmids and the large size of the plasmids compared to the chromosome, the borrelial plasmids may be more accurately described as minichromosomes (1, 26).

The mechanisms of replication and segregation of the chromosome and plasmids in *B. burgdorferi* remains largely unexplored. The completed *B. burgdorferi* genome sequence identified a limited complement of genes encoding proteins involved in DNA replication, repair, and recombination, similar to the genomes of *Mycobacterium genitalium* and *Treponema pallidum* (25-27). Recently, the chromosome's origin of replication was mapped to the center of the molecule between the *dnaA* and *dnaN* genes (70). The centrally located origin of replication and the identification of plasmid dimers (52) suggests that replication of the linear molecules proceeds through a circular intermediate (Figure 1). If this model is correct, then the *Borrelia* have solved the end replication problem by initiating replication of linear molecules at a centrally located origin that results in the formation of a circular double-stranded intermediate. Subsequent cleavage at or near the telomeric sequences creates two linear molecules. The mechanism proposed above would conceivably require the assembly of multiprotein complexes for DNA replication and telomere resolution. Such complexes may involve proteins unique to *Borrelia* to either complete replication or to assemble the replication complex.

Figure 1

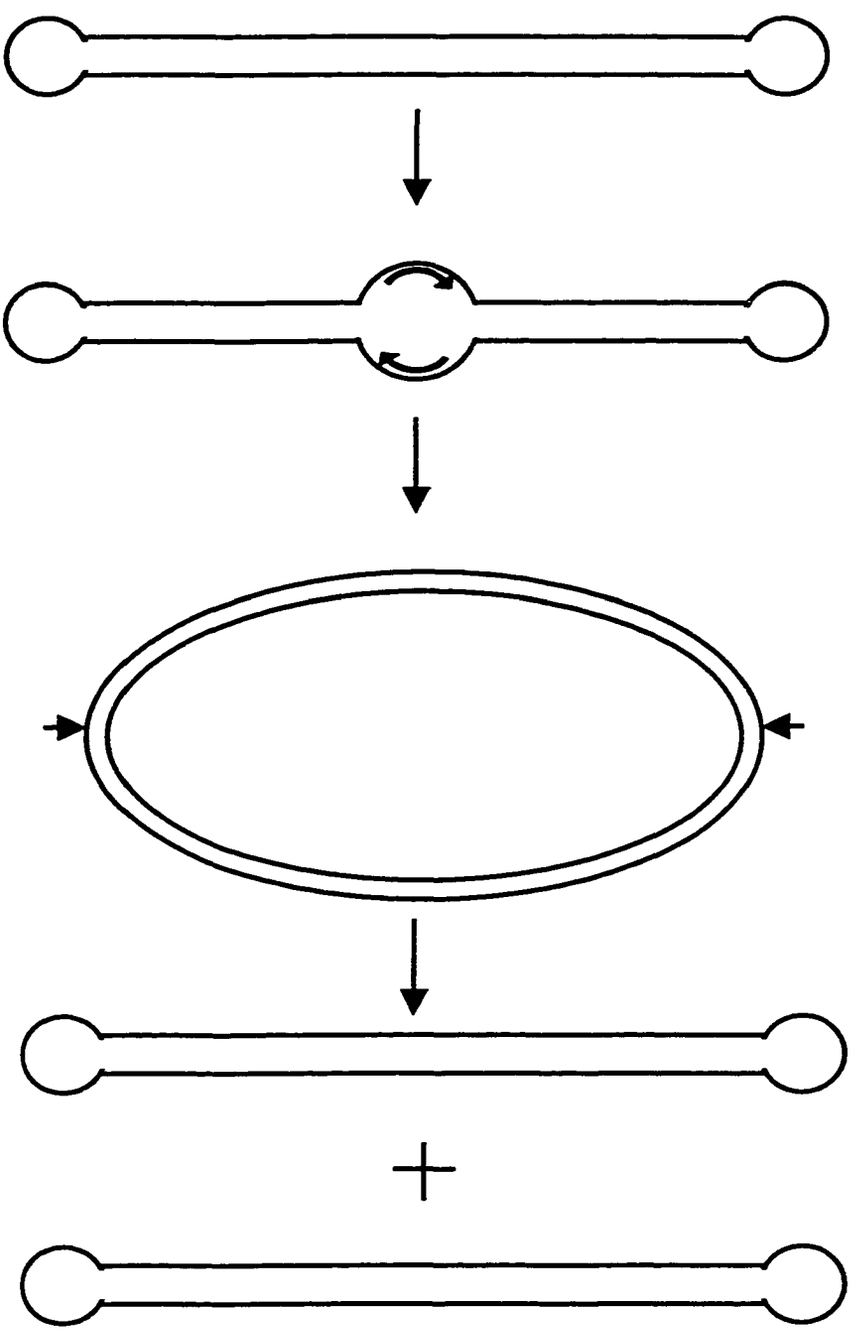

Figure 1. Putative replication mechanism for linear replicons (52, 70). Replication initiates at a centrally located origin, creating a circular intermediate. The joined telomeres are resolved by enzymatic cleavage (small arrows), resulting in two linear molecules.

1.2 DNA topology.

In addition to likely possessing novel mechanisms for DNA replication, *B. burgdorferi* may also have unique methods to regulate other DNA transactions, including chromosome condensation, transcription, and recombination. DNA topology is a crucial component in these processes and is likely to be important in the metabolism of the predominantly linear genome of *B. burgdorferi*. Linking number (ΔLk) is a measure of supercoiling; it is defined as the number of times two DNA strands in a closed-circular DNA molecule cross each other (3). ΔLk values are either positive or negative, depending on whether a helix is overwound or underwound compared to a right-handed relaxed DNA molecule and can only be altered by the breaking and resealing of the phosphodiester backbone (3).

Topology can be described by the equation:

$$\Delta Lk = \Delta Tw + \Delta Wr$$

where Tw is the twist, which is equivalent to helical pitch, and Wr is the writhe, which describes how the two strands of the helix coil around each other (3). Writhe is often associated schematically and intuitively with the concept of supercoiling. Changes in ΔLk arise from the helix being either wound around itself, generating plectonemic supercoiling, or by wrapping around a surface, creating toroidal supercoiling (3). In toroidally wrapped DNA, ΔLk remains constant unless the DNA backbone is broken and subsequently resealed. Therefore, when a DNA molecule is wrapped around a protein without breaking the phosphodiester backbone, twist and writhe must change in a way that compensate each other according to the equation above.

Both plectonemic and toroidal supercoiling have important roles in DNA metabolism. Both forms of supercoiling are critical in chromosome condensation in eukaryotes and in the compaction of the prokaryotic nucleoid, which is negatively supercoiled in the cell (3). In a more specific reaction, negative supercoiling stabilizes the complex formed between DnaA and *oriC* at the origin of replication on the *E. coli* chromosome (28). Negative supercoiling is not only needed to stabilize this interaction, but is also required for DnaA-dependent unwinding of the AT-rich region near the origin (9). Other processes requiring unwinding of duplex DNA are likewise enhanced by negative supercoiling, including transcription and recombination (50, 90).

1.3 Topoisomerases.

The class of enzymes known as topoisomerases regulate intracellular supercoiling levels, affecting both DNA topology and organization (100). These enzymes alter DNA supercoiling by catalyzing interconversions between different topological forms of DNA (100). The topoisomerases are grouped into three subfamilies: type IA, type IB, and type II. Type I enzymes catalyze DNA interconversions by introducing a single strand break into the helix, changing the linking number in steps of one (100). Type II enzymes introduce double strand breaks in the DNA substrate, changing the linking number in steps of two (100). Each topoisomerase has a different cellular function. However, some activities are shared among the enzymes, including the ability to relax negatively supercoiled DNA, which is common to all the topoisomerases (100).

DNA gyrase, an A_2B_2 heterotetramer, is a type II topoisomerase found solely in prokaryotes. It is the only topoisomerase capable of introducing negative supercoiling into closed-circular DNA (17, 30, 73, 100). The A and B subunits of DNA gyrase (GyrA

and GyrB) are encoded by *gyrA* and *gyrB*, respectively (38, 73). The enzyme has been well studied, and its structure and function is highly characterized because of its unique supercoiling activity and interaction with antimicrobial agents (73). The introduction of negative supercoiling by DNA gyrase has a variety of functions in the cell, including the removal of positive supercoils ahead of macromolecular complexes traversing a double-stranded helix and the condensation of the chromosome (50, 73).

DNA gyrase introduces negative supercoiling in an ATP-dependent manner. The N-terminal domain of GyrB contains the ATPase activity, and the C-terminal domain interacts with GyrA to stabilize the tetramer (73). GyrA contains the DNA breakage-reunion activity in the N-terminal domain and the DNA-binding activity in the C-terminal domain (73). The introduction of negative supercoiling is dependent on the wrapping of a 140-bp DNA segment around the enzyme with positive writhe, creating negative writhe elsewhere in the molecule (49, 73). The wrapping of DNA around DNA gyrase is critical to the function of the enzyme. Wrapping mostly occurs around the C-terminal domain of GyrA (72). Removal of the C-terminal domain abolishes the wrapping of DNA around the enzyme and eliminates the introduction of negative supercoiling, although not other enzymatic activities (40).

After DNA wraps around the enzyme, DNA gyrase cleaves both strands of the DNA substrate, covalently attaching the 5′ ends of each DNA strand to the enzyme through transesterfications to two tyrosine residues (73). The double-strand break serves as a gate for the passage of another segment of double-stranded DNA (75). ATP hydrolysis likely drives the conformational changes in the enzyme that are necessary to

pass the DNA substrate through the center of the tetramer (75, 100). The break is resealed after strand passage, resulting in the introduction of two negative supercoils.

B. burgdorferi has genes encoding a type I topoisomerase (*topA*), and two type II topoisomerases (*gyrA*, *gyrB*, *parC*, and *parE*) (26, 38). Pharamacological studies indicate the presence of a DNA gyrase activity in *B. burgdorferi*, and circular plasmids isolated from the spirochete are negatively supercoiled (84). What role, if any, DNA gyrase has in the metabolism of the linear DNA molecules in the organism is unknown.

1.4 Accessory Proteins.

DNA condensation. Naked supercoiled DNA molecules are in a dynamic state in solution, with constant fluctuations occurring in the twist and writhe (45). Intracellularly, however, changes in twist and writhe may be limited due to constraint induced by DNA-binding proteins (65). Toroidal supercoiling *in vivo* plays a large role in DNA metabolism and condenses DNA more efficiently than plectonemic supercoiling (6). The best example of DNA condensation by toroidal supercoiling is the eukaryotic nucleosome, where DNA is highly ordered and deformed into a compact conformation. In the nucleosome, a 145-bp DNA segment is wrapped in 1.8 left-handed superhelical turns around a histone core (34). This amount of helix distortion in the nucleosome is not obtainable in solution without bending or wrapping the helix around a protein, indicating the importance of protein-DNA interactions in chromosome compaction (97).

An ordered nucleosome structure has not been identified in prokaryotes; however, a more loosely ordered nucleoid containing toroidally supercoiled molecules has been described (31, 57). A number of small basic DNA-binding proteins have been identified that associate with the bacterial nucleoid, including HU, integration host factor (IHF),

Fis, and H-NS. Though none of these proteins are found in the cell in sufficient quantities to package DNA into a nucleosome structure, they can stabilize nucleoid packaging (97). These proteins condense DNA by either introducing sharp bends into the DNA molecule, or by wrapping the helix around a protein core. The major protein found associated with the *E. coli* nucleoid is the HU protein, which is more thoroughly described below (78, 98).

B. burgdorferi may have a different mechanism for packaging DNA than other prokaryotes due to the presence of linear DNA molecules. A large degree of compaction is obtained by negatively supercoiling a closed-circular molecule. Unlike circular molecules, *B. burgdorferi* linear replicons are not topologically constrained and cannot maintain plectonemic supercoiling when naked in solution. However, the linear molecules of *B. burgdorferi* may contain supercoiled domains *in vivo* that assist in genome compaction. For example, supercoiling in the middle of the chromosome is unlikely to be relieved by the untwisting of the DNA ends 500 kb away, creating a localized region of supercoiling. DNA-binding proteins bound to the linear replicons may assist in creating and maintaining these supercoiled domains, similar to the supercoiled domains found in eukaryotic chromatin. Another possibility is that toroidal supercoiling has a larger role in compacting the *B. burgdorferi* genome than plectonemic supercoiling. Repeating filaments resembling eukaryotic nucleosomes are observed in gently lysed *E. coli* (31). Similar structures have also been observed with linear DNA molecules, indicating that a topologically constrained molecule is not necessary to package DNA into a nucleoid structure (13, 20).

DNA chaperones. DNA deformation induced by small DNA-binding proteins not only assists in packaging the chromosome into a nucleoid structure but also functions in the assembly of nucleoprotein complexes. Complex structures consisting of multiple protein-DNA and protein-protein interactions are the functional machinery that carry out DNA-transactions (21, 22). Small DNA-binding proteins that function as accessory proteins or DNA chaperones often facilitate the assembly of these multi-protein DNA-binding complexes. These proteins promote formation of higher-order nucleoprotein complexes and aid in the localized deformation of DNA by melting, bending, or wrapping the helix (65).

DNA chaperones are similar to protein chaperones that stabilize a polypeptide in a conformation that mediates proper folding of a protein. DNA chaperones bend or twist DNA into a conformation that can be more easily assembled into a nucleoprotein complex (97). These proteins bind without sequence specificity and bind cooperatively, altering DNA conformation along a required length. Binding to DNA stabilizes the helix, facilitating the recruitment of other proteins to the bent, wrapped, or curved conformation. This chaperone-DNA interaction is dynamic, allowing regulatory proteins to readily displace the chaperones in some instances. The deformation of the helix by a chaperone can also bring two or more proteins bound at distant sites on a DNA molecule into closer proximity. Protein-protein contacts that occur between chaperones and regulatory proteins may also be important in establishing a functional complex (91).

DNA chaperones often recognize the shape of the helix or localized distortions not necessarily due to a specific DNA sequence. DNA has intrinsic flexibility, with some sequences being more flexible than others. Repeating sequences consisting of at least

four bp of A or T nucleotides repeated every 10 to 11 bp are highly bendable (32). The binding of an accessory protein more easily deforms these flexible sites. DNA supercoiling distorts the helix and forms double-stranded crossovers that may be analogous to bent or cruciform DNA structures, which many accessory proteins prefer to bind *in vitro* (97).

Upon bending, the major and minor groove on the concave surface become more compact, while the grooves on the convex surface are expanded (68). During this process, many proteins interact with the sugar-phosphate backbone through ionic interactions and hydrogen bonds. Other proteins interact with the bases through hydrophobic interactions (67). Some chaperones, including HU and IHF, bind the minor groove and are thought to intercalate between the bases to introduce a bend into the helix. The DNA-binding domain of HMG-1, a eukaryotic DNA chaperone, contains one amino acid that intercalates between adjacent basepairs, resulting in the untwisting of the helix, which is compensated by a reduction in writhe (41). HMG-1 functions analogously to the *E. coli* HU protein, and its method of bending the helix may be similar to the interaction between HU and DNA .

HU and IHF. The two most highly characterized prokaryotic DNA chaperones are HU and IHF, which have already been briefly described. These two proteins were first identified for their roles in bacteriophage metabolism (64, 79). They are abundant in *E. coli*, with concentrations of 30,000 dimers and 8,500-17,000 dimers per cell, respectively (19, 64, 79). Many bacteria encode separate HU and IHF proteins; however, some prokaryotes, such as *Bacillus subtilis*, synthesize a single protein that functions in both roles (61).

IHF is a heterodimer in *E. coli*, consisting of two subunits: IHF-α (M_r = 11,224) and IHF-β (M_r = 10,581) encoded by *himA* and *hip* (*himD*), respectively. IHF binds DNA at specific sites with the consensus sequence PyAANNNNTTGAT-A/T (69). The affinity of the interaction ranges from 1 x 10^{-9} M to 2 x 10^{-8} M (29). Binding of IHF introduces bends up to 140° into DNA (63). The sharp bends introduced by IHF binding change the DNA conformation, but have little effect on topology, as bends in the helix arise in a way that twist and writhe compensate each other (63).

The sequences of HU and IHF are 45% identical to each other and in many reactions one protein can substitute for the other (69). However, despite the similarity between the two proteins, they interact with DNA quite differently. HU exists as a dimer of non-identical subunits: HU-α (M_r = 9535) and HU-β (M_r = 9225) encoded by *hupA* and *hupB*, respectively (69). HU can, however, function as a homodimer, and in many organisms the protein exists as a dimer of identical subunits (20). HU binds weakly and nonspecifically to RNA, single-stranded DNA, and double-stranded DNA (63). The binding of HU to DNA toroidally supercoils the molecule, introducing negative writhe (11).

HU is the prototypical example of a bacterial DNA chaperone: it interacts weakly with DNA (K_d = 1.3 x 10^{-5} M), deforms the helix upon binding, and binds without sequence specificity (7, 11). HU stabilizes untwisted DNA molecules promoting the assembly of nucleoprotein complexes for DNA packaging and facilitating DNA melting required for replication, recombination, and transcription initiation (7) . The role of HU has been highly characterized in Mu transposition, which is described in more detail below.

1.5 Mu transposition.

Bacteriophage Mu transposition is a model system for examining prokaryotic DNA chaperone activity in assembling complex nucleoprotein structures. Transposons are mobile DNA elements that "jump" from one location to another. The *in vitro* system for bacteriophage Mu transposition is well-defined and requires a series of coordinated protein-protein and protein-DNA interactions on a supercoiled substrate (Figure 2) (15). The Mu transposon consists of three *cis*-acting sequences including the enhancer and two ends termed left and right, with each end containing multiple transposase binding sites (15). Two *trans*-acting factors are encoded by the Mu transposon: the Mu A transposase and Mu B. The Mu A transposase promotes strand cleavage and joining at the two ends of the transposon, and Mu B enhances Mu A activity and inhibits self transposition (15). The host contributes two DNA chaperones to the reaction: HU and IHF, which function as accessory proteins in assembling transposition intermediates known as transpososomes (15).

Mu transposition requires cleavage of the transposon from the donor and the insertion of the transposon into a new site. In the first step of the reaction, Mu A, HU, and IHF in the presence of Mg^{2+} bind the Mu transposon located on a supercoiled substrate. HU introduces a bend in the donor molecule at the left end of the transposon, and IHF binds and bends the enhancer region. HU binds DNA nonspecifically under most circumstances. However, in Mu transposition, HU binds at a precise 83-bp region at the left end of the transposon (47, 48). HU also binds at least one other site during transposition that has not yet been specifically identified (46). The transpososome formed between the donor molecule, Mu A, HU, and IHF is termed the LER complex; it

Figure 2

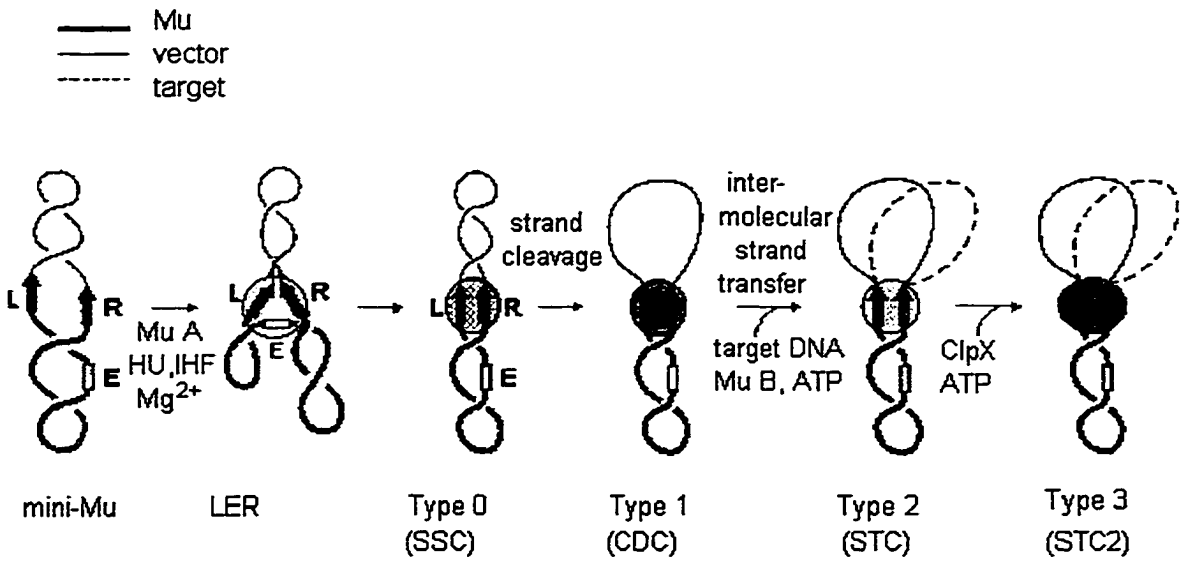

Figure 2. Mu transposition intermediates (15).

is rapidly converted to the Type 0 complex (102). In this transpososome, Mu A is correctly positioned on the donor molecule to induce cleavage. Mu A-mediated strand cleavage forms the Type 1 complex, leaving 3′-OH groups at each end of the Mu transposon. Intermolecular strand transfer of the 3′ ends into a new random location occurs in the presence of Mu B, resulting in the Type 2 complex. Finally, the Type 3 complex is formed through the action of ClpX, a protein chaperone that introduces a conformational change in the Type 2 transpososome and mediates disassembly of the complex.

1.6 The *B. burgdorferi* GyrA C-terminal domain.

Hbb, an HU/IHF homolog in *B. burgdorferi*, was previously identified and shown to substitute for both HU and IHF using a genetic complementation assay in *E. coli* based on bacteriophage lambda growth (95). Here, we identify and characterize a second small DNA-binding protein unique to *B. burgdorferi*. The C-terminal domain of the A subunit of DNA gyrase is naturally synthesized in *B. burgdorferi* as an abundant 35-kDa DNA-binding protein, separate from the subunits that compose DNA gyrase (Figure 3). This is a rare expression system for a prokaryotic cellular genome and is the first example of a domain of DNA gyrase being naturally synthesized as a separate functional protein.

The GyrA C-terminal domain closely links the activities of the topoisomerases, particularly DNA gyrase, to DNA chaperones. The function of the GyrA C-terminal domain has been examined *in vitro* with the Mu transposition system and *in vivo* using a bacteriophage Mu complementation assay. We have found that the GyrA C-terminal domain, though not homologous, functions analogously to the HU protein of *E. coli*.

Figure 3

Figure 3. Schematic of full-length GyrA and the naturally synthesized GyrA C-terminal domain from *B. burgdorferi*. GyrA is a 91-kDa protein, and the GyrA C-terminal domain is 35 kDa. The GyrA C-terminal domain is identical in sequence to the C-terminal 311 amino acids of GyrA as indicated by the diagonal lines.

The identification, synthesis, and HU-like activity of the GyrA C-terminal domain is presented in chapter 3, and the activity of the internal promoter located within *gyrA* is described in chapter 4. The interaction of the GyrA C-terminal domain with DNA, including conformational changes in the helix induced by binding, is examined in chapter 5. We speculate that the GyrA C-terminal domain has a role in the metabolism of the linear chromosome and plasmids in *B. burgdorferi*. To begin to address this possibility, we have disrupted synthesis of the GyrA C-terminal domain in *B. burgdorferi* and are examining the phenotype of these spirochetes, which is discussed in chapter 6.

Chapter 2.

Materials and Methods

2.1 Chapter 3 methods.

GyrA C-terminal Domain Purification. A crude lysate of high passage *B. burgdorferi* strain B31 was prepared from an 18 L culture grown in BSK-H medium (Sigma) at 32°C as previously described (55) with the following modifications. Cells from a 1.5 L culture (in three 500 ml bottles) were collected at 10,500 x g for 20 min in a GSA rotor. The cell pellet was washed twice in 30 ml Dulbecco's phosphate-buffered saline (dPBS). Cells were collected in an SS34 rotor at 7500 x g for 10 min after the first wash and at 6000 x g for 10 min after the second wash. Cells were resuspended in 1.5 ml of TS (50 mM Tris-HCl, pH 8.0, 15% sucrose) and stored at -80°C. Twelve 1.5 ml aliquots of B31 were thawed at 37°C and pooled into six separate 3 ml aliquots. DTT (final concentration 2 mM), EDTA (final concentration 1 mM), and PMSF (final concentration 0.5 mM) were added to each aliquot. Nucleic acid was precipitated by slowing adding 1/5 the volume of 1 M KCl and 2/5 the volume of 5% streptomycin sulfate (pH 7.2 with NH_4HCO_3), followed by rotation at 4°C for 10 min. The lysate was clarified by centrifugation at 7,500 x g for 10 min in an SS34 rotor. The clarified lysate was dialysed against 20 mM Tris-HCl, pH 8 (the pH of Tris solutions was measured at 25°C), 0.5 mM EDTA, 10% glycerol (H buffer) (all dialysis steps were overnight at 4°C), and loaded onto a 5 ml Econo-Pac Heparin Cartridge (Bio-Rad). The column was eluted with a 100 ml linear gradient from 0-1 M NaCl in H buffer at 2 ml min^{-1} and twenty five fractions (4 ml each) were collected. Fractions containing the 35-kDa protein (which eluted at 440 mM-520 mM NaCl) were dialysed against 10 mM sodium phosphate, pH

6.8, 10% glycerol, and loaded onto a 2 ml CHT2-I hydroxyapatite column (Bio-Rad). The column was eluted with a 20 ml linear gradient from 10-500 mM sodium phosphate, pH 6.8, in 10% glycerol, followed by a 10 ml linear gradient from 500-1000 mM sodium phosphate, pH 6.8, in 10% glycerol at 1 ml min^{-1}. Thirty fractions (1 ml each) were collected. Fractions containing the 35-kDa protein (which eluted at ~ 700 mM sodium phosphate) were dialysed against 10 mM sodium phosphate, pH 6.8, 0.5 mM EDTA, 10% glycerol (P buffer) and loaded onto a 1 ml Mono-S column (Pharmacia). The column was eluted with a 15 ml linear gradient from 0-0.5 M NaCl in P buffer, followed by a 5 ml linear gradient from 0.5-1 M NaCl in P buffer at 1 ml min^{-1}. Twenty-five fractions (1 ml each) were collected. Fractions containing the 35-kDa protein (which eluted at ~650 mM NaCl) were pooled and mixed with an equal volume of 3.4 M $(NH_4)_2SO_4$, 100 mM sodium phosphate, pH 7, 10% glycerol, 1 mM EDTA, and loaded onto a 1 ml Phenyl Superose column (Pharmacia). The column was eluted with 15 ml of a 1.7-0 M $(NH_4)_2SO_4$, and 50-10 mM sodium phosphate, pH 7, linear gradient in 10% glycerol, 1 mM EDTA at 0.5 ml min^{-1}. The flow-through, which contained the 35-kDa protein, was dialysed against 50 mM Tris-HCl, pH 7.5, 0.1 M KCl, 0.1 mM EDTA, 5 mM DTT, 50% glycerol, and stored at -20°C. See section 2.3 for purification of the recombinant GyrA C-terminal domain from *E. coli*.

Electrophoretic Mobility Shift Assay (EMSA). A 255-bp PCR product amplified from the 17-kb linear plasmid beginning 23 bp from the left end was used as an EMSA substrate. The substrate was prepared as previously described (55) using the following primers kindly provided by K. Tilly: 10 pmol of primer TL16g end-labeled with [γ-^{32}P]-dATP and 25 pmol of primer TL16h (Table 1). The end-labeled DNA

substrate was gel-purified from a 5% polyacrylamide gel (29:1 acrylamide:bis) by soaking the excised gel slice containing the substrate in STE (10 mM Tris-HCl, pH 8.0, 1 mM EDTA, 100 mM NaCl) overnight at 37°C. The purified substrate was concentrated by ethanol precipitation and resuspended in TE (10 mM Tris-HCl, pH 8.0, 1 mM EDTA). Approximately 2.1 μg of labeled DNA was incubated in a 15 μl reaction at 25°C for 30 min with the 35-kDa GyrA C-terminal domain in 10 mM HEPES, pH 7.5, 90 mM KCl, 300 μg ml^{-1} BSA, 200 μg ml^{-1} poly-dIdC, 10% glycerol. DNA-protein complexes were resolved by electrophoresis through a 4% polyacrylamide gel (80:1 acrylamide:bis) and visualized by autoradiography.

Generation of a polyclonal antiserum. Recombinant *B. burgdorferi* GyrA C-terminal domain (250 μg in dPBS) was injected into an eight week-old female New Zealand White rabbit with Freund's complete adjuvant (FCA). A total volume of 500 μl consisting of the GyrA C-terminal domain and FCA was mixed in two syringes connected by a micro emulsifying needle for approximately 15 min. The mixture was injected subcutaneously into four quadrants in the rabbit's hip and shoulder. A second injection was repeated two weeks later as above, except Freund's incomplete adjuvant was used. Subsequent injections were carried out every week using 10 μg of recombinant protein in dPBS injected intravenously in the ear. Serum was collected after 4 weeks and analyzed for GyrA C-terminal domain specific antibody by Western analysis.

Immunoblots. Whole cell *B. burgdorferi* lysates were prepared by boiling cells in SDS-PAGE loading buffer (125 mM Tris-HCl, pH 6.8, 4% SDS, 20% glycerol, 1.4 M 2-mercaptoethanol, 0.2% bromphenol blue). The GyrA C-terminal domain was prepared

as described above and boiled in SDS-PAGE loading buffer. Samples were fractionated by 7.5% SDS-PAGE. For Western analysis, samples were transferred to a PVDF membrane (Immobilon P, Millipore) and incubated with rabbit antiserum raised to a recombinant GyrA C-terminal domain, followed by goat antibody to rabbit immunoglobulin G conjugated with horseradish peroxidase (Bio-Rad). The band size and intensity were determined using a Gel Doc 1000 system with Multi Analyst software (Bio Rad).

RNA Analysis. Total RNA was isolated from 100 ml cultures using 15 ml of TRIzol™ reagent as described by the manufacturer (Gibco BRL). Fifteen μg of total RNA in 50% formamide, 1X MOPS (20 mM MOPS, 5 mM sodium acetate, 1 mM EDTA, pH 7.0), and 2.2% formaldahyde was heated at 55°C for 15 min. RNA samples were at a final volume of 28 μl, to which 1 μl of 0.5 mg ml^{-1} EtBr and 1 μl of loading buffer (50% glycerol, 1mM EDTA, 0.25% bromphenol blue, 0.25% xylene cyanol) were added. RNA was fractionated on 1.2% formaldehyde-agarose gels (1.2% SeaKem agarose, 1X MOPS, and 1.1% formaldahyde) in 1X MOPS running buffer at 80 V. Following electrophoresis, the gel was rinsed with two changes of H_2O for 5 min each. RNA was transferred to nylon membranes (Hybond N^+, Amersham) using a vacuum blotter with H_2O for 10 min, denaturation buffer (50 mM NaOH, 10mM NACl) for 10 min, neutralization buffer (0.5 mM Tris-HCl, pH 7.5, 1.5 M NaCl, 1 mM EDTA) for 10 min, and 20X SSC (1X SSC is 0.15 M NaCl and 0.015 M sodium citrate [pH 7.0]) for 3 h. Membranes were UV crosslinked using a Stratalinker (Stratagene). Membranes were either incubated for one hour in prehybridization solution (hybridization solutions described below without labeled probe), or dried and rehydrated in 6X SSC.

Hybridization with oligonucleotide probes was performed as previously described (53). Oligonucleotides (150 ng) were end-labeled with [γ-^{32}P]-dATP using T4 polynucleotide kinase and purified by passage through G25 spin columns (Boehringer-Mannheim). Labeled oligonucleotides were incubated with membranes in hybridization solution A (1M NaCl, 1X P Buffer [50 mM Tris, pH 7.5, 1% SDS, 2 mg ml^{-1} BSA, 2 mg ml^{-1} PVP, 2 mg ml^{-1} ficoll, 1 mg ml^{-1} sodium pyrophosphate], 10% dextran sulfate and 100 µl salmon sperm DNA) overnight at 32°C. Membranes were washed twice with 2X SSC-0.1% SDS for 10 min each at 32°C, washed once with 0.2X SSC-0.1% SDS for 1 h at 32°C, wrapped in cellophane, and exposed overnight.

Hybridization with PCR probes was performed as previously described (10). PCR probes were labeled with [α-^{32}P]-dATP and Prime-It® II Random Primer Labeling Kit according to the manufactures instructions (Stratagene). Probes were incubated with membranes in hybridization buffer B (5X SSC, 1% SDS, 5X Denhardt's, 50% formamide, and 100 µl salmon sperm DNA) overnight at 42°C. Membranes were washed twice with 2X SSC-0.1% SDS for 10 min each at 25°C, washed once with 0.2X SSC-0.1% SDS for 1 h at 42°C, wrapped in cellophane, and exposed overnight. The band intensity and size were determined using an Image Acquisition and Analysis system (Ambis) and a Gel Doc 1000 system with Multi Analyst software (Bio Rad), respectively.

Primer extension was used to map the RNA 5′ ends for the 1200-nt transcript encoding the GyrA C-terminal domain, and the 5000-nt transcript encoding GyrB and GyrA. One pmol of end-labeled primer was incubated with 7 µg of total cellular RNA in 50 mM KCl, 10 mM Tris-HCl, pH 8.3, 5 mM $MgCl_2$, 1 mM each dNTP, and 20 U RNase inhibitor. Extension was

performed at 42°C with 50 U of MuLV reverse transcriptase. Extension products were resolved on a 6% polyacrylamide sequencing gel, and sizes were determined by use of a DNA sequencing ladder. Two different primers were used in the primer extension assay to map the transcriptional start sites for the 1200-nt transcript: *gyrA* 1510R and *gyrA* 1547R. Primer *gyrB* U26R was used to map the transcriptional start sites for the 5000-nt transcript.

Mu donor cleavage reaction. Mini-Mu donor plasmid pBL07, HU, IHF, and Mu A were kindly provided by G. Chaconas. Type 1 *in vitro* reactions were performed as previously described with all reaction components at twice the standard concentrations (62). Type 1 reactions (30 μl) contained 6 μg ml^{-1} Mu A, 7.5 μg ml^{-1} HU, 0.4 μg ml^{-1} IHF, 30 μg ml^{-1} pBLO7 in 25 mM HEPES-NaOH, pH 7.6, 10 mM $MgCl_2$, 140 mM NaCl. The GyrA C-terminal domain, when substituted for HU, was used at a concentration of 7.5 μg ml^{-1}. After incubation at 30°C for 5 min, the reactions were divided into equal aliquots and 1% SDS was added to one aliquot. Reactions were resolved on 1% agarose gels at 80 V for 3 h in 1X TAE buffer. Gels were stained with ethidium bromide (0.5 μg ml^{-1}) for 30 min, and destained in H_20 for 30 min.

Complementation. The portion of the *gyrA* gene encoding the GyrA C-terminal domain, including the promoter, was cloned into the plasmid vector pCR.2.1-TOPO (Invitrogen). Primers *gyrA* 1213F and *gyrA* 2433R+*Sph*I were used to PCR-amplify nucleotides 1213-2433 of *gyrA* from *B. burgdorferi* strain B31. The 1220-bp product was cloned into the vector resulting in plasmid pTASK1 (Table 2) according to the manufacturer's instructions and transformed into TOP10F' *E. coli* cells (Invitrogen). Plasmid pTASK1 was isolated and transformed into competent *E. coli* strain A5196

(*hupA hupB*) (59). Synthesis of the 35-kDa GyrA C-terminal domain in *E. coli* strain A5196 was confirmed by Western analysis as described above using 12.5% SDS-PAGE.

Induction of Mu *cts*62 lysogens (kindly provided by K. Drlica) and preparations of lysate were performed as previously described (12). *E. coli* strain KD1028 was grown in LB Mg (LB supplemented with 2.5 mM $MgSO_4$) at 32°C to a density of 1-4 x 10^8 cells ml^{-1}. Mu was induced by incubating the culture at 44°C in a water bath for 25 min. Induced cultures were allowed to further lyse by growing at 37°C for 2 h (complete lysis was rare). Chloroform (50 µl ml^{-1}) was added to induced cultures and cell debris removed by centrifugation after mixing. Mu dilutions were made in LB Mg (Mu is unstable in solution and must be prepared fresh for each experiment). Mu titers were measured by plaque formation on N99 lawns at 37° C on 1% LB Ca Mg plates (LB supplemented with 1mM $CaCl_2$, 2.5 mM $MgSO_4$) with 0.5% LB top agar. The efficiency of plating (e.o.p.) was measured as the ratio of bacteriophage Mu titer on the mutant strain to the titer on the wild-type strain.

2.2 Chapter 4 methods.

Plasmids. The promoter for the gene encoding the GyrA C-terminal domain, containing all three transcriptional start sites, was PCR-amplified from *B. burgdorferi* strain B31 using primers *gyrA* 1213F and *gyrA* 1459R (Table 1). Amplification was performed with 1 cycle of 94°C for 1 min, 25 cycles of 92°C for 30 sec, 58°C for 30 sec, and 72°C for 30 sec, and 1 cycle of 72°C for 5 min. The 246-bp product was ligated into plasmid pCR.2.1-TOPO to create plasmid pTAPGAC.1 (Table 2). The *gyrA C-terminal domain* promoter was excised by *Eco*RI digestion, gel-purified, and ligated into the *Eco*RI restriction site of plasmid pGOΔ1 (88), creating plasmid pGOΔGAC. Clones were

selected on LB agar containing 10 μg ml^{-1} chloramphenicol. Correct orientation of the promoter was confirmed by PCR amplification using primers *gyrA* 1459R and KS, which yields an ~250-bp product if the promoter is in the correct orientation, and primers *gyrA* 1213F and KS, which result in an ~300-bp product when the promoter is in the reverse orientation.

To create plasmid pGOΔGAC 1213-1418, the 5′ portion of the *gyrA C-terminal* domain promoter consisting of only the first transcriptional start site was PCR-amplified from *B. burgdorferi* strain B31 using primers *gyrA* 1213F and *gyrA* 1418R. Amplification was performed with 1 cycle of 94°C for 1 min, 25 cycles of 92°C for 30 sec, 42°C for 30 sec, and 72°C for 30 sec, and 1 cycle of 72°C for 5 min. The 205-bp product was ligated into plasmid pCR.2.1-TOPO, resulting in plasmid pTAGyrA 1213-1418. The promoter region was cloned into pGOΔ1 as described above, to create plasmid pGOΔGAC 1213-1418. Correct orientation of the promoter was confirmed using the method described above, except primer *gyrA* 1418R was used in place of *gyrA* 1459R.

In order to maintain the reporter construct in *E. coli* containing either plasmids pExGAC or pTASK1, an approximately 1-kb fragment including the *gyrA C-terminal domain* promoter and *cat* gene from plasmid pGOΔGAC was cloned into plasmid pACYC177, which contains an origin of replication from plasmid p15A. Plasmid pGOΔGAC was digested with *Cla*I followed by treatment with Mung Bean Nuclease. The approximately 1-kb fragment containing the *gyrA C-terminal domain* promoter and *cat* gene was excised by digestion with *Bam*HI. This fragment was cloned into plasmid pACYC177 at the *Ban*I-*Bam*HI site that had been modified after digestion with *Ban*I with

Mung Bean Nuclease to create a blunt end. Cloning into the *Ban*I-*Bam*HI site of pACYC177 disrupted the amp^r gene located on the plasmid.

Minimal inhibitory concentration (MIC) determinations. LB agar plates with chloramphenicol at 0, 2.5, 5, 10, 20, 40, 80, 160, 320, and 640 μg ml^{-1} were used for MIC determinations. *E. coli* in mid-log phase were diluted in LB broth, and approximately 10^4 bacteria in 10 μl volumes were spotted on plates. Plates were incubated overnight at 37°C, and the MIC of chloramphenicol was the lowest concentration that prevented visible growth.

2.3 Chapter 5 methods.

Cloning and Purification of the GyrA C-terminal domain. The gene encoding the GyrA C-terminal domain was PCR-amplified from *B. burgdorferi* strain B31 using primers *gyrA* 1498F+*Nsi*I, which introduced an *Nsi*I restriction site upstream of the Ser^{500} codon, and *gyrA* 2433R+*Sph*I, which introduced a *Sph*I restriction site downstream of the translational stop codon (Table 1). Amplification was performed with 1 cycle of 94°C for 1 min, 25 cycles of 92°C for 30 sec, 47°C for 30 sec, and 72°C for 1 min, and 1 cycle of 72°C for 7 min. The 947-bp PCR product was cloned into pCR2.1 (Invitrogen) resulting in plasmid pTAGAC.2 (Table 2). Digestion of plasmid pTAGAC.2 with *Nsi*I followed by treatment with Mung Bean Nuclease created a blunt 5′ end. Digestion with *Sph*I excised the fragment encoding the GyrA C-terminal domain. The fragment was gel purified and ligated into the gel-purified ~4.5-kb fragment derived from plasmid pTTQ18* (kindly provided by Tony Maxwell), which was generated by digestion with *Eco*RI, Mung Bean Nuclease, and *Sph*I, sequentially (72). The resulting plasmid,

pExGAC, was transformed into competent *E. coli* strain JM109 and sequenced to confirm the correct reading frame.

E. coli strain JM109 transformed with plasmid pExGAC was grown at 37°C in 2xYT media containing 50 μg ml^{-1} carbenicillin. Expression was induced at an optical density of 0.5 at 595 nm by the addition of isopropyl-β-thiogalactopyranoside (IPTG) to a final concentration of 0.5 mM. Cells were harvested 4 hours after induction by centrifugation. The cell pellet was resuspended in 20 mM Tris-HCl, pH 8.0, 0.5 mM EDTA, 0.2 mM dithiothreitol, 0.5 mM phenylmethylsulfonyl fluoride, and 10% glycerol. Cells were lysed by sonication, and the lysate was clarified by centrifugation at 10,000 x *g* for 10 min. Soluble cellular components were precipitated by a 70% (w/v) ammonium sulfate fractionation and collected by centrifugation at 10,000 x *g* for 10 min. The supernatant, containing the majority of the GyrA C-terminal domain, was dialyzed three times against 1 L of 20 mM Tris-HCl, pH 8.0, 0.5 mM EDTA, and 10% glycerol. The GyrA C-terminal domain was purified to apparent homogeneity by passage over heparin, Mono-S, and hydroxyapatite columns as described above (section 2.1). The GyrA C-terminal domain was stored at -20°C in 50 mM Tris-HCl, pH7.5, 0.1 M KCl, 0.1 mM EDTA, 5 mM dithiothreitol, and 50% glycerol.

Electrophoretic mobility shift assays (EMSAs). The 300-bp EMSA substrate was prepared by amplifying the first 300 bp from the coding sequence of *ospC* from *B. burgdorferi* strain B31 as described above (section 2.1) using 10 pmol of primer *ospC* 1F end-labeled with [γ-^{32}P]-dATP and 25 pmol of primer *ospC* 300R. The end-labeled DNA substrate was gel-purified from a 5% polyacrylamide gel (29:1 acrylamide:bis) by soaking the excised gel slice containing the substrate in STE (10 mM Tris-HCl, pH 8.0, 1

mM EDTA, 100 mM NaCl) overnight at 37°C. The purified substrate was concentrated by ethanol precipitation and resuspended in TE (10 mM Tris-HCl, pH 8.0, 1 mM EDTA). The 101-bp linear and circular substrates were prepared as described below. Reactions were resolved on either 4% or 10% polyacrylamide gels (80:1 acrylamide:bis) as described above.

Filter binding assays. Filter binding assays were performed as previously described with the following modifications (89). A 300-bp DNA fragment from the coding sequence of *ospC* was PCR-amplified from *B. burgdorferi* strain B31 using the primers above, end-labeled with [γ-^{32}P]-dATP, and gel-purified.

Dilutions of the GyrA C-terminal domain were made in BB (10 mM HEPES, pH 7.5, 90 mM KCl, 50 μg ml^{-1} BSA) in a final volume of 20 μl. The protein was added to 180 μl of 10 mM HEPES, pH 7.5, 90 mM KCl (FBB) containing 10 pmol of end-labeled DNA and incubated at 23°C for 30 min. Aliquots of 180 μl were filtered through presoaked nitrocellulose membranes (Millipore HAWP, 0.45 um) at 10 mbar. Membranes were immediately washed with 5 ml of FBB and then dried at 60°C for 20 min. DNA retained on the membranes was quantified by scintillation counting. Background retention, measured in the absence of the GyrA C-terminal domain, was approximately 3% of the total input DNA. Background was subtracted and the percentage of input DNA retained on the filter calculated. The K_d was determined by plotting the percentage of DNA retained on the membrane as a function of the natural logarithm of the protein concentration (89).

DNA bending assays. The ability of the GyrA C-terminal domain to bend DNA was assayed by DNA circularization experiments (71). The 101-bp DNA bending

substrate was prepared by PCR-amplifying an 84-bp fragment from the coding sequence of *gyrB* from *B. burgdorferi* strain B31 using primers *gyrB* 1F and *gyrB* 84R. The 84-bp fragment was cloned into pCR2.1-Topo (Invitrogen) according to the manufacturer's instructions resulting in plasmid pCirc. Digestion of pCirc with *Eco*RI excised a 101-bp fragment containing 84 bp of *gyrB*. The 101-bp fragment was gel-purified by agarose gel electrophoresis followed by extraction using a Qiaex II kit (Qiagen), and end-labeled with [γ-^{32}P]-dATP using T4 polynucleotide kinase.

The 101-bp labeled substrate (10 nM) was incubated with the GyrA C-terminal domain at the indicated concentrations for 30 min at 23°C in 50 mM Tris-HCl, pH 7.5, 10 mM $MgCl_2$, 10 mM dithiothreitol, 1 mM ATP, 25 $\mu g\ ml^{-1}$ BSA, and 6% glycerol. T4 DNA ligase (400 U) was added to the binding reaction, and samples were incubated for 16 h at 16°C. Protein was removed by organic extraction, and the DNA was concentrated by ethanol precipitation. Reactions were fractionated on 6% polyacrylamide gels (29:1 acrylamide:bis) and visualized by autoradiography. For restriction enzyme analysis, the 101-bp circle was gel purified as described above. Restriction digests were analyzed on 15% polyacrylamide gels (29:1 acrylamide:bis) and visualized by autoradiography.

DNA-wrapping assay. The DNA-wrapping activity of the GyrA C-terminal domain was examined as previously described with the following modifications (72). Nicked pBR322 (13.3 ng μl^{-1}) was incubated with the GyrA C-terminal domain at 25°C for 30 min in 50 mM Tris-HCl, pH 7.5, 55 mM KCl, 2 mM $MgCl_2$, 5 mM dithiothreitol, and 5% glycerol. Nicks were sealed by incubation with T4 DNA ligase (400 U) and 1 mM ATP at 25°C for 60 min. Protein was removed by organic extraction, and the DNA

was concentrated by ethanol precipitation. Reactions were resolved on 1% agarose gels and stained with ethidium bromide.

Two dimensional agarose gel electrophoresis was used to determine if the resulting topoisomers were positively or negatively supercoiled (84). Electrophoresis in the first dimension was performed under native conditions on a 1% agarose gel. The gel was soaked 16 h in 1.3 μM chloroquine, rotated 90°, and electrophoresed in the second dimension. The gel was soaked in H_2O to remove chloroquine and then stained with ethidium bromide.

2.4 Chapter 6 methods.

Construction of a plasmid to disrupt synthesis of the GyrA C-terminal domain. An approximately 4-kb fragment encoding the 5′ 301 bp of *dnaA*, *gyrB*^{r}, and the 5′ 1521 bp of *gyrA* was PCR-amplified from *B. burgdorferi* B31-NGR using primers *dnaA* 301R and *gyrA* 1521R/GACKO with Taq + Precision (Stratagene) (Table 1). Primer *gyrA* 1521R/GACKO was a mutagenic primer that introduced point mutations into the *gyrA C-terminal domain* ribosome binding site, mutated the ATG initiation codon to a Leu residue, and mutated Met^{503} of *gyrA* to an Ile residue. Mismatches in primer *gyrA* 1521R/GACKO used for site directed mutagenesis are underlined in Table 1. Amplification was performed with 1 cycle of 94°C for 1 min, 25 cycles of 92°C for 30 sec, 50°C for 30 sec, and 72°C for 4 min, and 1 cycle of 72°C for 15 min. The product was concentrated, and primers plus unincorporated nucleotides were removed using a Wizard PCR Prep (Promega). The purified PCR product (2 μl) was incubated in a 10 μl reaction containing 1X PCR buffer (Sigma), 2.5 mM $MgCl_2$, 10 mM ATP, and 1 U of

Taq polymerase (Sigma) to adenylate the 5′ ends. The adenylated product was cloned into plasmid pCR.2.1-TOPO, creating plasmid pTAKO1 (Table 2).

A 900-bp fragment encoding the GyrA C-terminal domain was PCR-amplified from NGR-B31 using primers *gyrA* 1462F/GACKO and *gyrA* 2362R with Taq + Precision. Primer *gyrA* 1462F/GACKO was a mutagenic primer that introduced the complementary mutations as described above for primer *gyrA* 1521R/GACKO. Mutagenic mismatches are underlined in Table 1. Amplification was performed with 1 cycle of 94°C for 1 min, 25 cycles of 92°C for 30 sec, 55°C for 30 sec, and 72°C for 1 min, and 1 cycle of 72°C for 7 min. The amplification product was purified as described above, 5′ ends were adenylated, and the product cloned into plasmid pCR.2.1-TOPO, to create plasmid pTAKO2.

The mutagenic plasmid for disrupting synthesis of the GyrA C-terminal domain was constructed by ligating the approximately 800-bp *Spe*I fragment from plasmid pTAKO2 into *Spe*I-digested plasmid pTAKO1, resulting in plasmid pGACKO. Mutations were confirmed by DNA sequencing.

***B. burgdorferi* transformation and screening clones.** Preparation of competent *B. burgdorferi* strain B31, electroporation, and plating of spirochetes was performed as previously described (83). Plasmid pGACKO (0.5 - 7μg) was transformed into competent *B. burgdorferi* strain B31 by electroporation. Cells were recovered for 20 h in BSK medium and plated in the presence of 0.5 μg ml^{-1} coumermycin A_1. The amount of culture plated varied from 0.1 ml to 8.9 ml.

Coumermycin A_1-resistant (cou^r) clones were screened by PCR using a 20 μl reaction volume and primers *gyrA* 1492F/GACKOSC and *gyrA* 2362R. PCR conditions

were 1 cycle of 94°C for 1 min, 30 cycles of 92°C for 30 sec, 56°C for 30 sec, and 72°C for 1 min, and 1 cycle of 72°C for 7 min. Colonies were picked from plates with sterile toothpicks and added to amplification reactions (76). PCR products were analyzed by agarose gel electrophoresis and visualized with Gel STAR (FMC Bioproducts). Positive colonies were cultured by transferring the agarose containing the colony with a sterile Pasteur pipette to liquid medium.

Table 1. Oligonucleotides.

Name	Sequence (5′-3′)
dnaA 301R	AAGTTTCGTTAAGAGCCG
gyrA 1213F	AAAGATGCAAGGGAGAGGC
gyrA 1462F/GACKO	ATAATTTATGATGAAGAAGTTTTAAAAACTAGTCTTT-CGGATTTAATTCAAAAAGAAAAT
gyrA 1492F/GACKOSC	AGTCTTTCGGATTTAATT
gyrA 1498F+*NsiI*	ATGCATCGGATTTAATGCAAAAAG
gyrA 1393R	TCCTTACTGGATTCAAGAG
gyrA 1418R	GTTTCTTCTCTTATAATATTAATA
gyrA 1459R	TAGTTCGACGTTCATCGCC
gyrA 1480R	CCTCCTCATCATAAATTATTTTAG
gyrA 1510R	GCATTAAATCCGACATAC
gyrA 1521R/GACKO	ATTTTCTTTTTGAATTAAATCCGAAAGACTAGTTTTT-AAAACTTCTTCATCATAAATTAT
gyrA 1547R	CCTTTCTTTGTAAGCATAACAAC
gyrA 2362R	CTTTGCCTTGTTCAGATAC
gyrA 2433R+*SphI*	AGCATGCTTATTTAATAAATTTTGA
gyrA 1441R	CAAATTTCAAACCTAAATTAATA
gyrB U26R	TCTAGACACAGATAAATTCTACATT
gyrB 1F	ATGAATTATGTTGCTAGTAACATT
gyrB 84R	AACTGAGCCTATATACATGCCAGG
KS	CGAGGTCGACGGTATC
ospC 1F	ATGAAAAAGAATACATTAAGTGCG
ospC 300R	TCCCGCTAACAATGATCCATTGTG
TL16g	AGACTAATAAAATAATGAATA
TL16h	GTATTTTGACTCAAAACTTTA

Table 2. Plasmids.

Plasmid	Function	Reference
pGOΔ1	Parent plasmid containing *cat* reporter gene.	(88)
pGOΔ5	*ospA* promoter.	(88)
pGOΔGAC	*gyrA C-terminal domain* promoter.	This work.
pGOΔGAC 1213-1418	*gyrA C-terminal domain* promoter.	This work.
pTAPGAC.1	promoter subclone.	This work.
pTAGyrA 1213-1418	promoter subclone.	This work.
pTTQ18*	Expression plasmid.	(72)
pRJR79	*E. coli* GyrA C-terminal domain expression.	(72)
pExGAC	GyrA C-terminal domain expression.	This work.
pTAGAC.2	GyrA C-terminal domain subclone.	This work.
pBLO7	Mini-Mu.	(102)
pTASK1	GyrA C-terminal domain expression.	This work.
pKK55	Hbb expression.	(95)
pCirc	101-bp *Eco*RI fragment.	This work.
pKD101	HU expression.	K. Drlica.
pSK001	Promoter clone.	This work.
pTAKO1	Knockout subclone.	This work.
pTAKO2	Knockout subclone.	This work.
pGACKO	Knockout clone.	This work.

Chapter 3

Natural synthesis of an HU-like protein from the C-terminal domain of DNA gyrase in *Borrelia burgdorferi*

(Adapted from Knight and Samuels, in revision for *EMBO J.* 1999)

We report here that, in addition to synthesizing a functional DNA gyrase consisting of full-length GyrA and GyrB subunits, *B. burgdorferi* also synthesizes the C-terminal domain of GyrA as a distinct and abundant 35-kDa DNA-binding protein. This unique protein forms a higher-order nucleoprotein complex, substituting for HU in Mu transposition *in vitro*, and functions analogously to HU *in vivo* to support bacteriophage Mu growth in *E. coli*.

Identification of the GyrA C-terminal domain. The 35-kDa GyrA C-terminal domain was identified in a biochemical screen for telomere-binding proteins in *B. burgdorferi*. A whole cell lysate was fractionated by heparin column chromatography, and fractions were screened for telomere-binding activity by electrophoretic mobility shift assays (EMSAs) using a sub-telomeric DNA fragment (Figure 4A and B). A DNA-binding activity localized to fractions containing a 35-kDa protein, which was further purified to apparent homogeneity (Figure 4A). N-terminal sequencing identified the 35-kDa protein as the GyrA C-terminal domain, encompassing residues 500-810 of the full-length GyrA protein (Figure 4C).

The large amount of the 35-kDa protein isolated and the presence of a methionine codon, which could serve as a translational start codon, directly upstream of the N-terminal serine residue (Figure 4C) suggested that the protein was synthesized as a distinct protein independent of full-length GyrA. To determine if the GyrA C-terminal

Figure 4

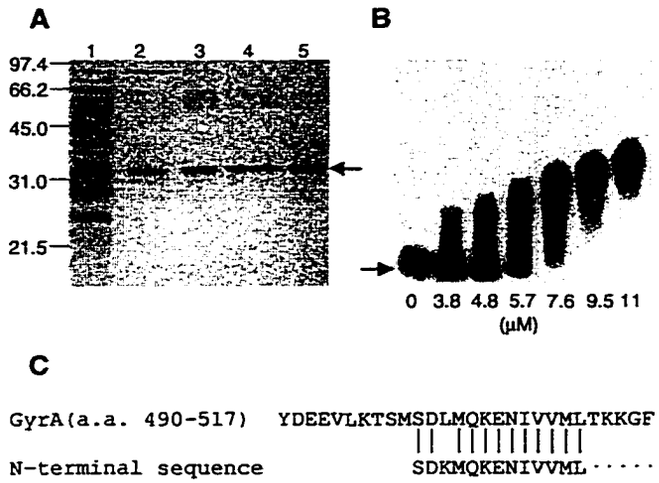

Figure 4. Identification of the GyrA C-terminal domain. (**A**) Purification of the 35-kDa GyrA C-terminal domain. Silver-stained 12.5% SDS-PAGE gel following the purification of the 35-kDa protein to apparent homogeneity. The clarified lysate was prepared from strain B31 (lane 1), and fractionated over heparin (lane 2), hydroxyapatite (lane 3), Mono S (lane 4), and Phenyl Superose (lane 5) columns. Molecular mass standards shown in kilodaltons. (**B**) EMSA. Increasing amounts of the 35-kDa protein incubated with an end-labeled DNA fragment. The arrow indicates migration of unbound DNA. (**C**) N-terminal sequence of the 35-kDa protein and alignment with GyrA. The N-terminal sequence is aligned with residues 490-517 of GyrA, predicted from the DNA sequence (BB0435; GenBank accession number AE001148) (26). Lines represent identity determined by sequencing; dots indicate predicted identity.

domain was present in intact cells, or if the protein arose as a result of proteolytic cleavage during purification, whole cell *B. burgdorferi* lysates were examined by immunoblot analysis using a polyclonal antiserum to a recombinant *B. burgdorferi* GyrA C-terminal domain (Figure 5). The antiserum detected the 35-kDa GyrA C-terminal domain and a ~91-kDa protein, predicted to be full-length GyrA. The 35-kDa protein was present in crude lysates at a 5 to 20-fold higher level than the 91-kDa protein. The cellular concentration of the GyrA C-terminal domain was estimated to be 34,000 molecules per cell based on regression analysis of a standard curve generated from immunoblots with known concentrations of the GyrA C-terminal domain (data not shown).

Analyses of the transcripts encoding the GyrA C-terminal domain. To determine if the 35-kDa protein was expressed in *B. burgdorferi* as a novel gene product, we used Northern analysis to identify a transcript encoding the GyrA C-terminal domain. When using a probe specific for the 3′ end of *gyrA*, encoding the C-terminal 310 amino acid residues, two separate transcripts were detected: a 1200-nucleotide (nt) and a 5000-nt transcript (Figure 6A and B). The 1200-nt transcript is large enough to encode the GyrA C-terminal domain (310 amino acids); however, it is not large enough to encode full-length GyrA (810 amino acids). A probe specific for the 5′ end of *gyrA*, encoding the N-terminal domain of GyrA, only hybridized with the 5000-nt transcript (data not shown). We hypothesize that the larger transcript is a bicistronic message encoding both GyrB (634 amino acids) and GyrA. This is supported by the hybridization of a *gyrB*-specific probe to the 5000-nt transcript (Figure 6C). As shown in Figure 6A, *gyrB* is located directly upstream of *gyrA*, with only 14 bp separating the two genes (26, 38).

Figure 5

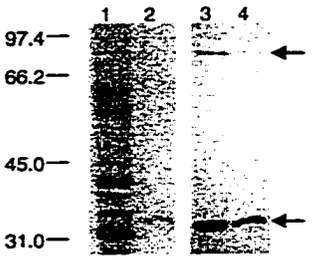

Figure 5. Western analysis. Proteins were resolved by 7.5% SDS-PAGE. Lanes 1 and 3, whole cell *B. burgdorferi* lysate; lanes 2 and 4, purified GyrA C-terminal domain. Lanes 1 and 2 were stained with Coomassie brilliant blue. Lanes 3 and 4 were Western blotted and probed with anti-GyrA C-terminal domain antiserum. The arrows indicate the putative full-length 91-kDa GyrA (top) and the 35-kDa GyrA C-terminal domain (bottom). Molecular mass standards shown in kilodaltons.

Figure 6

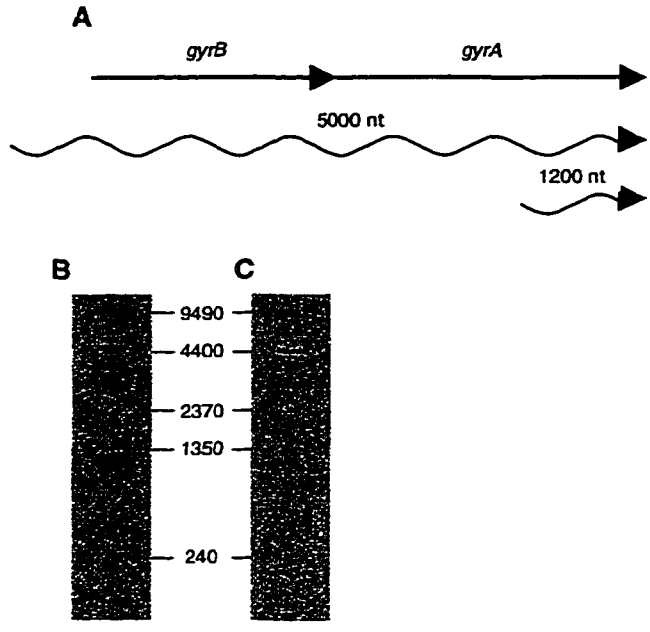

Figure 6. Northern analysis. (**A**) Schematic of *gyrB* (2.0 kb) and *gyrA* (2.4 kb) genes located on the chromosome, the bicistronic transcript (5000 nt) encoding both GyrB and GyrA proteins, and the monocistronic transcript (1200 nt) encoding the 35-kDa protein (DNA shown as solid arrow, RNA as wavy arrow). (**B**) Northern blot of total cellular RNA probed with a PCR product specific for the 3′ end of *gyrA* encoding the 35-kDa GyrA C-terminus. (**C**) Northern blot of total cellular RNA probed with a PCR product specific for the *gyrB* coding sequence. Molecular size standards shown in nucleotides.

The 1200-nt transcript is expressed at a four-fold higher level than the larger bicistronic message as assayed by quantifying the hybridization signals. We have also identified the GyrA C-terminal domain-specific transcript in a number of other species of *Borrelia* including *B. garinii*, *B. afzelii*, and the relapsing fever spirochete *B. hermsii*, which all contain predominantly linear genomes (data not shown).

Transcriptional start site analysis of the GyrA C-terminal domain specific mRNA. Primer extension analysis was used to locate three putative transcriptional start sites for the 1200-nt transcript located at nts 1412, 1430, and 1435 of *gyrA* (Figure 7A). The presence of multiple transcriptional start sites is not uncommon in either *B. burgdorferi* genes or small DNA-binding protein genes from other prokaryotes (43, 53, 95). Although promoter sequences in *B. burgdorferi* have not been functionally defined, only the transcriptional start site at nt 1412 has upstream sequences that resemble sigma 70 consensus promoters (Figure 7B). The absence of a consensus promoter sequence upstream of transcriptional start sites at nts 1430 and 1435 is perhaps not unexpected, considering that the regions upstream of all three transcriptional start sites not only serve as regulatory sequences for transcription, but must maintain the open reading frame for full-length GyrA. Two direct repeats of TATTAAT are also found in the promoter region (Figure 7B).

To confirm that the three identified sites were in fact 5′ ends of transcripts, we used a series of oligonucleotides flanking the three sites as probes in Northern hybridizations (Figure 7C). Five oligonucleotide probes complementary to regions downstream of the transcriptional start site at nt 1435 all hybridized with both the 5000-nt and 1200-nt transcripts. However, two oligonucleotide probes complementary to regions

Figure 7

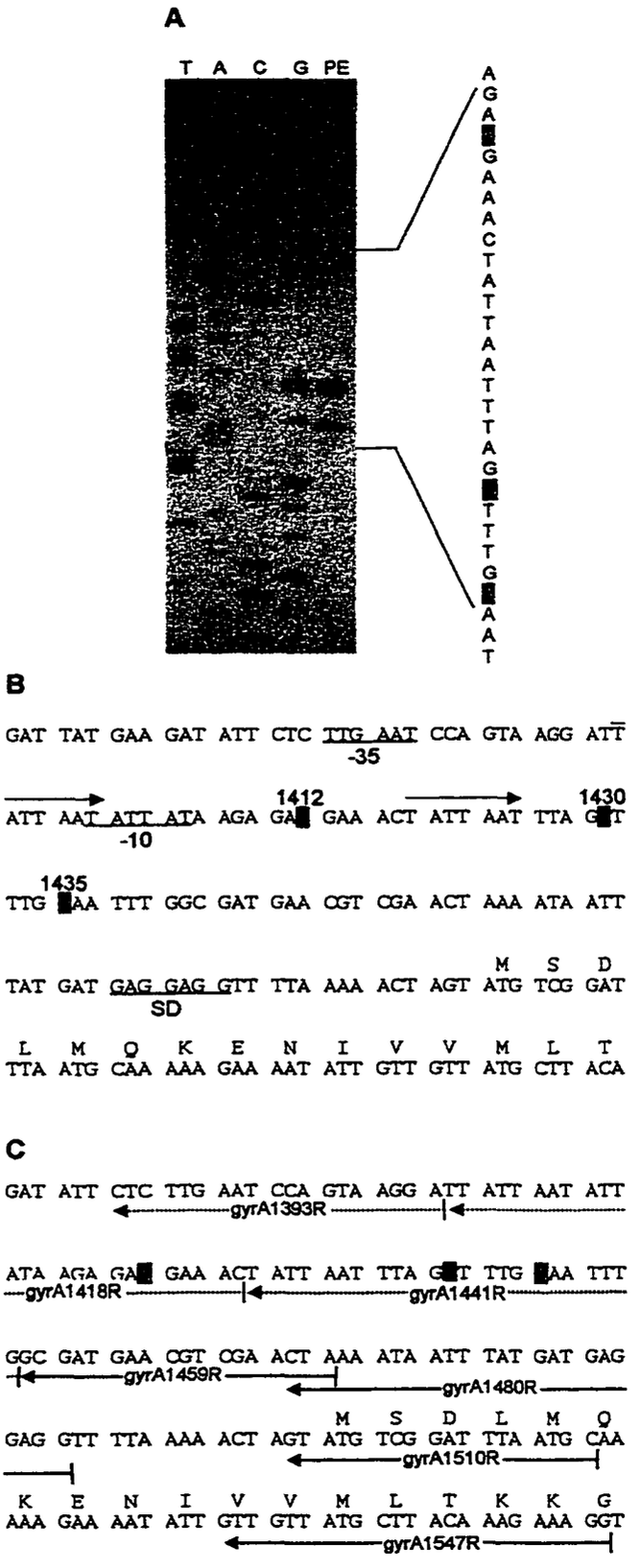

Figure 7. Transcriptional start site identification. (**A**) Primer extension mapping of three RNA 5′ ends using primer *gyrA* 1510R. Transcriptional start sites are indicated in inverted typeface. Two separate primers (*gyrA* 1510R and *gyrA* 1547R) identified the same three 5′ ends in three independent isolations of B31 RNA (data for *gyrA* 1547R not shown). (**B**) Putative regulatory sequences. Transcriptional start sites are numbered and in inverted typeface. Possible -10, -35, and Shine-Dalgarno (SD) sequences are underlined. Two direct repeats are indicated with arrows. Amino acid residues of the GyrA C-terminal domain coding sequence are indicated above the appropriate codon. (**C**) Schematic representation of oligonucleotide probe hybridization. Nucleotides 1369-1548 of *gyrA* are shown. Arrows indicate oligonucleotides complementary to the sense strand. Solid arrows indicate oligonucleotides that hybridize with the 1200-nt transcript, and dashed arrows indicate oligonucleotides that do not hybridize with the 1200-nt transcript. Transcriptional start sites determined by primer extension are shown in inverted typeface. Amino acid residues of the GyrA C-terminal domain are indicated above the appropriate codon.

upstream of transcriptional start sites at nts 1430 and 1435 hybridized only with the 5000-nt transcript. Oligonucleotide probe gyrA1441R, complementary to the region directly downstream of the transcriptional start site at nt 1412, also failed to hybridize with the 1200-nt transcript, suggesting that nt 1412 is not used as often as the other two transcriptional start sites under standard culture conditions. These data are consistent with the primer extension data, which indicate that nt 1430 serves as the major transcriptional start site (Figure 7A). The identified promoter region including all three transcriptional start sites for the 1200-nt transcript functions in *E. coli* to regulate expression of a reporter gene (Chapter 4) and to produce a functional GyrA C-terminal domain as described below (Figure 10).

We also mapped two putative transcriptional start sites for the bicistronic message encoding *gyrA* and *gyrB*, using primer extension. RNA 5′ ends were identified at 149 and 126 nucleotides upstream of the putative ATG initiation codon of *gyrB* (Figure 8). Upstream of both transcriptional start sites are -10 consensus sequences for a sigma 70 promoter. However, a -35 sigma 70 consensus sequence with the correct spacing is only found upstream of the transcriptional start site at 149 nucleotides upstream of the translational initiation codon. The arrangement of the promoter sequences is similar to the *gyrA C-terminal domain* promoter, with complete consensus sequences located upstream of only the most 5′ transcriptional start site. In *E. coli*, *gyrA* and *gyrB* are encoded on two separate transcripts. There is a consensus -10 sequence upstream of the transcriptional start sites for each gene, but both genes lack a consensus -35 sequence (60).

Figure 8

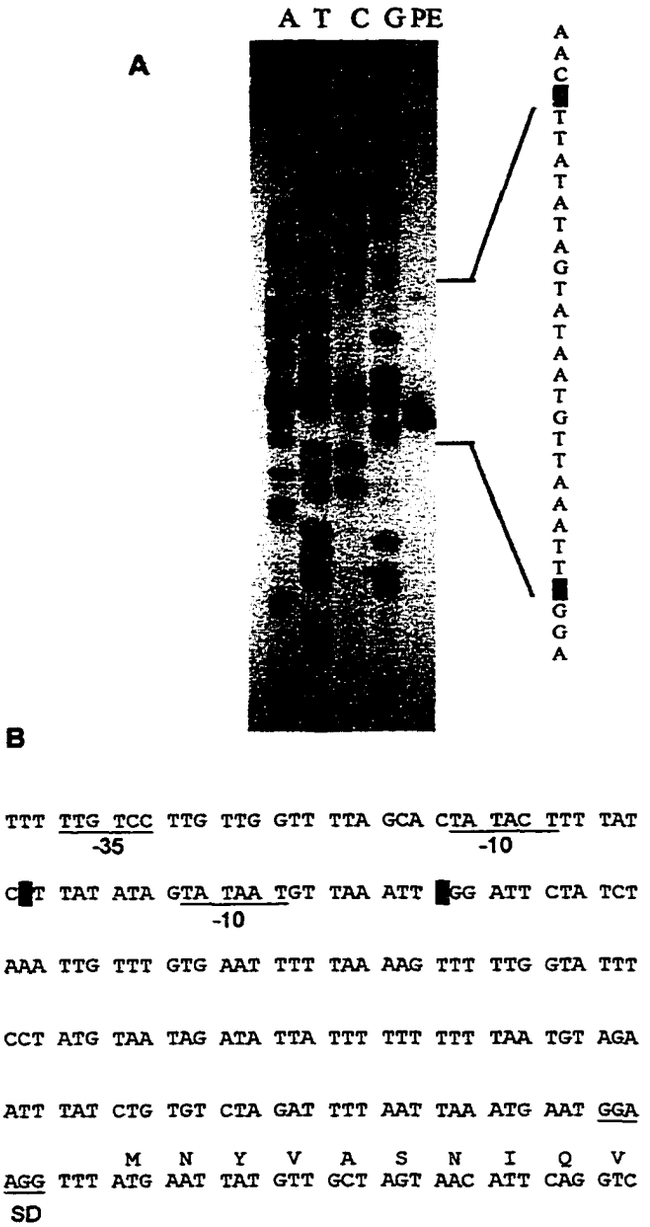

Figure 8. Transcriptional start site for the 5000-nt bicistronic message. (**A**) Primer extension mapping of two RNA 5′ ends using primer gyrB U26R. Transcriptional start sites are indicated in inverted typeface. (**B**) Putative regulatory sequences. Transcriptional start sites are numbered and in inverted typeface. Possible -10, -35, and Shine-Dalgarno (SD) sequences are underlined. Amino acid residues of the GyrB coding sequence are indicated above the appropriate codon.

Nucleoprotein complex formation. EMSAs were used to examine DNA-binding activity of the GyrA C-terminal domain. As the amount of protein added to the binding reaction was increased, the mobility of the DNA-protein complex was further retarded (Figure 4B). This indicates that multiple protein molecules are capable of binding to each DNA molecule. Similar results were obtained using the *ospAB* promoter sequence from the 50-kb linear plasmid, an *ospC* coding sequence from the 26-kb circular plasmid, and synthetic telomere sequences from the 17-kb linear plasmid, suggesting that the DNA-binding activity of the protein is nonspecific (data not shown and Figure 12).

Based on the abundance of the GyrA C-terminal domain and its non-specific DNA-binding activity, we hypothesized that the protein had an analogous function to the small DNA-binding protein HU of *E. coli*. An *in vitro* Mu transposition assay was used to test this hypothesis. The Type 1 complex is an early intermediate in the transposition reaction (Figure 2) and its formation is stringently dependent on the presence of HU (18). The GyrA C-terminal domain substituted for HU in the *in vitro* reaction, as assayed by the formation of the Type 1 complex in Mu transposition (Figure 9).

Complementation of an HU mutant. Genetic manipulation of *B. burgdorferi* is in the initial stages of development, which has been hindered by a complex, undefined medium and the availability of only one selectable marker (85). Therefore, we investigated the *in vivo* activity of the GyrA C-terminal domain in a more experimentally tractable system. The ability of the gene encoding the GyrA C-terminal domain to

Figure 9

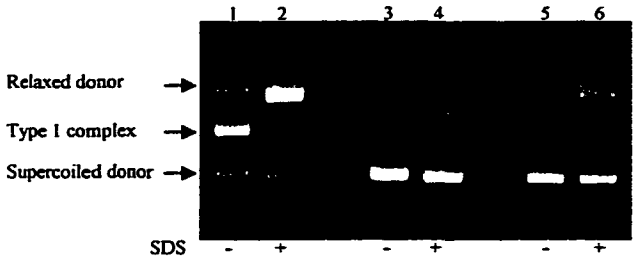

Figure 9. Mu donor-cleavage reaction. The supercoiled donor plasmid is converted to the Type 1 complex in the presence of HU, Mu A, and IHF. Mu A introduces two single strand nicks into the supercoiled plasmid. The introduction of single strand nicks does not result in a relaxed plasmid, due to the complex formed with Mu A, HU, and IHF, which separates the Type 1 complex into two separate topological domains: relaxed and supercoiled. In the presence of SDS, the proteins dissociate from the Type 1 complex, resulting in a nicked open circular plasmid. Lanes 1 and 2, with HU; Lanes 3 and 4, without HU; Lanes 5 and 6, GyrA C-terminal domain substituting for HU.

complement a bacteriophage Mu plating deficiency in an *E. coli hupA hupB* mutant (A5196) was examined. The GyrA C-terminal domain was expressed in *E. coli* A5196 from plasmid pTASK1 using the natural *B. burgdorferi* promoter within the *gyrA* gene. Synthesis of the GyrA C-terminal domain in *E. coli* was confirmed by Western analysis (Figure 10). *E. coli* containing pTASK1 restored Mu growth as assayed by efficiency of plating (e.o.p.). Bacteriophage Mu formed plaques approximately 10^4-fold more efficiently on the *hupA hupB* mutant in the presence of the GyrA C-terminal domain, restoring the Mu plating deficiency to wild type levels (Table 3).

Figure 10

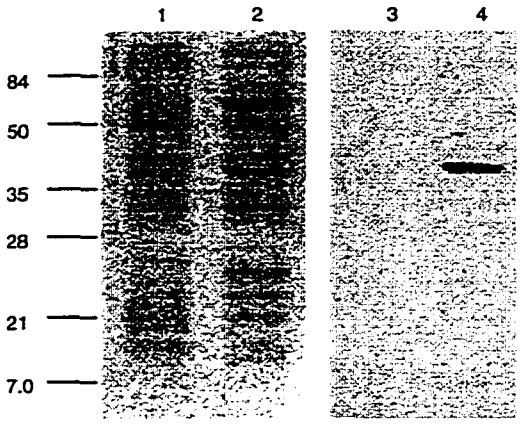

Figure 10. Expression of the *B. burgdorferi* GyrA C-terminal domain in *E. coli*. Lanes 1 and 3, whole cell *E. coli* strain A5196 lysate; lanes 2 and 4, whole cell *E. coli* strain A5196 containing plasmid pTASK1. Lanes 1 and 2 were stained with Coomassie brilliant blue. Lanes 3 and 4 were examined by Western analysis. Molecular mass standards shown in kilodaltons.

Table 3. Bacteriophage Mu growth

Strain	plasmid	e.o.p
N99	-	1
A5196 *hupA hupB*	-	$<4x10^{-5}$
A5196 *hupA hupB*	pTASK1	1

A5196 relevant genotype: *hupA 16*::*kan hupB11*::*cat* (Mendelson et al., 1991).

Chapter 4

Analysis of the promoter of the GyrA C-terminal domain-specific transcript

(Adapted from Knight, Alverson, and Samuels, in preparation)

Plasmid pGOΔ1 was previously constructed to examine transient promoter activity in *B. burgdorferi* (88). *B. burgdorferi* promoters assayed using this system are active in *E. coli* at a level that correlates to their activity in *B. burgdorferi* (88). Promoters from the *B. burgdorferi* genes *ospA*, *ospC*, and *flaB* have previously been examined (88). We analyzed the activity of the GyrA C-terminal domain promoter in *E. coli* using plasmid pGOΔ1 and the system developed by Sohaskey *et al.* (88).

Cloning the GyrA C-terminal domain promoter. A 246-bp fragment encoding the GyrA C-terminal domain promoter containing all three transcriptional start sites (Figure 11) was cloned into the reporter plasmid pGOΔ1 (resulting plasmid termed pGOΔGAC). The promoter contains a sigma 70 consensus -10 and -35 sequence, and two direct repeats (Figure 7B). The 3′ transcriptional start site at nucleotide 1435 is 39 nucleotides upstream of the ribosome binding site located on pGOΔ1. Plasmid pGOΔGAC 1213-1418 was constructed by cloning a 205-bp fragment containing only the transcriptional start site at nucleotide 1412 into pGOΔ1. The transcriptional start site on this plasmid is positioned 18 nucleotides upstream of the ribosome binding site.

Minimal inhibitory concentrations (MICs). Promoter activity was measured *in vivo* by MICs of chloramphenicol in *E. coli* containing either plasmid pGOΔGAC or plasmid pGOΔGAC 1213-1418. The activity of these *E. coli* was compared to *E. coli*

Figure 11

A

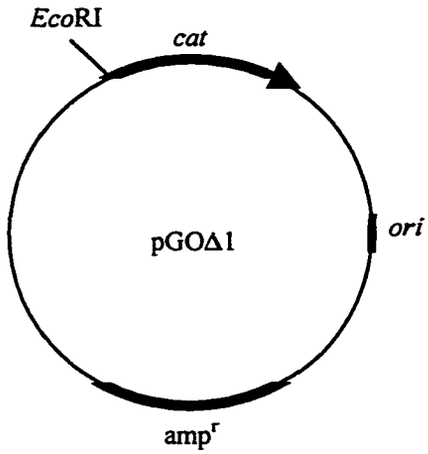

B

pGOΔGAC

*Eco*RI

GATTCCGCCCTTAAAGATGCAAGGGAGAGGCTTGTTTCGAATTTTGGTCTTTC

AGAGATTCAGGCCAATTCAGTTCTTGATATGAGGTTACAAAAACTTACAGCC

CTTGAGATTTTAAGCTTGAAGAGGAGCTTAATATACTGTTAAGCTTAATAAAA

GATTATGAAGATATTCTCTTGAATCCAGTAAGGATTATTAATATTATAAGAGA

AGAAACTATTAATTTAGGTTTGAAATTTGGCGATGAACGTCGAACTAAAAAG

*Eco*RI *cat*→

GGCGattcaggaggcatatcaaatg

pGOΔGAC 1213-1418

*Eco*RI

GATTCCGCCCTTAAAGATGCAAGGGAGAGGCTTGTTTCGAATTTTGGTCTTTC

AGAGATTCAGGCCAATTCAGTTCTTGATATGAGGTTACAAAAACTTACAGCC

CTTGAGATTTTAAGCTTGAAGAGGAGCTTAATATACTGTTAAGCTTAATAAAA

GATTATGAAGATATTCTCTTGAATCCAGTAAGGATTATTAATATTATAAGAGA

*Eco*RI *cat*→

AGAAACAAGGGCGattcaggaggcatatcaaatg

Figure 11. Reporter constructs. **(A)** Plasmid pGOΔ1 plasmid. Arrow indicates *cat* gene. The *Eco*RI restriction site directly upstream of the *cat* gene is shown. **(B)** Sequences of the cloned promoters from the *gyrA C-terminal domain.* Transcriptional start sites are shown in inverted type face, and predicted -10 and -35 sequences are underlined. Lower case type indicates the 5′ end of the *cat* gene on plasmid pGOΔ1 and includes the ATG start codon. The arrow indicates the direction of transcription.

containing plasmids pGOΔ1 (no promoter) and pGOΔ5 (*ospA* promoter). MICs of chloramphenicol demonstrated that the complete *gyrA C-terminal domain* promoter increased transcription of the *cat* reporter 16-fold higher than background levels of the *cat* gene without a promoter, and two-fold higher than the *ospA* promoter positive control (Table 4). The pGOΔ1 plasmid provided a low level of resistance to chloramphenicol (Table 4) due to a cryptic promoter, as previously reported (88).

Plasmid pGOΔGAC 1213-1418, which contained only the most 5′ transcriptional start site, conferred the same level of chloramphenicol resistance as plasmid pGOΔGAC containing the complete promoter. This suggests that the two promoter constructs have similar activity in *E. coli*. This is in contrast to the primer extension data reported in Chapter 2 (Figure 7), which indicates that the transcriptional start site at nucleotide 1412 is used less often than the other two downstream start sites.

The discrepancy between the MIC data and the primer extension data may be due to differences in the sensitivity of the two assays, or differences between promoter regulation in *E. coli* and *B. burgdorferi*. The primer extension data indicate only a slight difference in transcriptional start site preference. This slight variation may not be detectable with the less sensitive MIC assays. Alternatively, the differences between the two assays may be due to differences in flanking sequences in *B. burgdorferi* and plasmid pGOΔGAC.

Differences in the primer extension data and MIC data may also be explained by differences in regulatory *cis*-acting sequences or *trans*-acting factors. Plasmid pGOΔGAC 1213-1418 contains only one direct repeat element, whereas the complete

Table 4. MIC of chloramphenicol in *E. coli*.

Plasmid	Promoter	MIC μg ml^{-1} chloramphenicol
none	-	5
pGOΔ1	-	40
pGOΔ5	*ospA*	320
pGOΔGAC	*gyrA C-terminal domain*	640
pGOΔGAC 1213 -1418	*gyrA C-terminal domain*	640

promoter in *B. burgdorferi* contains the complete direct repeat. These direct repeats may be involved in regulation of promoter activity by recruiting a *trans*-acting transcription factor that represses transcription initiation at nucleotide 1412 in *B. burgdorferi*. The absence of one direct repeat element in plasmid pGOΔGAC 1213-1418 may not allow for the

recruitment of this putative repressor in *E. coli*, or the putative *trans*-acting factor may not be found in *E. coli*.

Effects of supercoiling in regulating the *gyrA C-terminal domain* promoter. DNA supercoiling is a global regulator of transcription and plays an important role in regulating the expression of a variety of genes (3). In particular, genes encoding the subunits of DNA gyrase in *E. coli* are regulated by the supercoiling level in the cell (60). We examined the effect of DNA supercoiling on expression of the *gyrA C-terminal domain* by growing *B. burgdorferi* in the presence of coumermycin A_1. Coumermycin A_1 is a coumarin DNA gyrase inhibitor that decreases intracellular supercoiling.

We examined the *gyrA C-terminal domain* gene expression in *B. burgdorferi* grown in coumermycin A_1 at the RNA level by Northern analyses and at the protein level by Western analyses. We did not observe a change in the expression level of either the 1200-nt GyrA C-terminal domain-encoding transcript or the larger 5000-nt bicistronic message encoding GyrB and GyrA over a range of 0 to 20 ng ml^{-1} coumermycin A_1 (data not shown). Similarly, GyrA C-terminal domain and GyrA synthesis, as assayed by Western analysis, did not change with increasing amounts of coumermycin A_1 (data not shown).

The effects of supercoiling in regulating the *gyrA C-terminal domain* promoter were also examined in *E. coli* containing plasmid pGOΔGAC. MICs of chloramphenicol were determined for *E. coli* containing the plasmid pGOΔGAC at coumermycin A_1 concentrations ranging from 0 to 1 μg ml^{-1}. The MIC of chloramphenicol remained at 640 μg ml^{-1} regardless of the coumermycin A_1 concentration (data not shown), indicating that DNA supercoiling is not a major determinant in regulating expression of the *gyrA C-terminal domain.*

Regulation of promoter activity by the GyrA C-terminal domain. We examined the ability of the *B. burgdorferi* GyrA C-terminal domain to regulate expression of its gene by expressing the GyrA C-terminal domain in *E. coli* containing the *gyrA C-terminal domain* promoter upstream of a reporter gene. The GyrA C-terminal domain was expressed from one of two different plasmids: pExGAC or pTASK1. Plasmid pExGAC contains an inducible promoter that can be regulated by IPTG levels, and plasmid pTASK1 constitutively expresses the gene encoding the GyrA C-terminal domain (Figure 10). The *gyrA C-terminal domain* promoter fused to the *cat* promoter gene from plasmid pGOΔGAC was cloned into plasmid pACYC177 to create plasmid pSK001. Moving the reporter construct into plasmid pACYC177 was necessary to ensure that both the reporter plasmid and the expression plasmid, which must have compatible replication mechanisms, would be maintained in *E. coli*. MICs of chloramphenicol were determined for *E. coli* containing plasmid pSK001 with either plasmids pExGAC or pTASK1. The MICs of chloramphenicol for these *E. coli* strains were compared to *E. coli* containing only plasmid pSK001. There was no difference between *E. coli* containing only the reporter plasmid and *E. coli* containing both the

reporter plasmid and one of the expression plasmids. *E. coli* containing plasmids pExGAC and pSK001 were grown in various amounts of IPTG to induce expression of the GyrA C-terminal domain, but this did not result in any differences in promoter activity. *E. coli* containing plasmid pSK001 had a lower MIC of chloramphenicol than *E. coli* containing plasmid pGOΔGAC, which is likely attributable to the lower copy number of plasmid pSK001. These data suggest that the GyrA C-terminal domain does not regulate expression of its own gene.

Chapter 5

Characterization of the GyrA C-terminal domain of *Borrelia Burgdorferi*: bending a linear genome

(Adapted from Knight and Samuels, in preparation)

The interaction between the *B. burgdorferi* GyrA C-terminal domain and DNA is described here. The GyrA C-terminal domain was cloned, overexpressed, and purified from *E. coli*. Using electrophoretic mobility shift assays and filter-binding assays, we have characterized the DNA binding activity of the protein. In addition, DNA conformational changes induced by GyrA C-terminal domain binding are examined.

Purification. The gene encoding the 35-kDa GyrA C-terminal domain was cloned into plasmid pTTQ18* downstream of a *tac* promoter (72). Over-production of the protein in *E. coli* was achieved as described in the 'Materials and Methods.' Ammonium sulfate fractionation of the crude lysate precipitated many of the cellular components, but the majority of the GyrA C-terminal domain remained soluble at 70% saturation (data not shown). The protein was further purified to apparent homogeneity by liquid chromatography using a modified method originally used in isolating the native protein from *B. burgdorferi*. Sequencing revealed an N-terminal Ser residue (data not shown), indicating that the N-terminal Met residue is post-translationally removed from the recombinant protein as well as the native protein. Gel filtration chromatography suggests that the GyrA C-terminal domain is a monomer in solution (data not shown).

DNA binding activity. The GyrA C-terminal domain from *B. burgdorferi* was originally isolated based on its DNA-binding activity (Figure 4). The protein binds DNA nonspecifically, with multiple protein molecules binding to each DNA molecule (Figure

4B). Further characterization of the DNA-binding activity of the *B. burgdorferi* GyrA C-terminal domain, in the absence of a nonspecific competitor DNA (poly-dIdC), shows that a stable DNA-protein complex forms at molar protein concentrations equal to and greater than the DNA concentration (Figure 12). Evidence of multiple protein molecules binding each DNA molecule is only observed at high molar ratios of protein to DNA. At an equal molar ratio of protein to DNA, the DNA is completely bound by the GyrA C-terminal domain, forming a distinct protein-DNA complex. This complex is the predominant species up to a 16-fold excess of protein, when a second, supershifted complex forms that migrates more slowly than the first. This supershifted complex is progressively retarded with increasing amounts of protein up to 1000 to 2000-fold molar excess. The original complex remains present at all protein concentrations, although the abundance of the complex gradually decreases as the protein concentration is increased.

Filter binding assays were used to determine the magnitude of the interaction for formation of the first complex observed by EMSAs. An apparent dissociation constant of 1×10^{-8} M was determined based on the protein concentration required to yield 50% maximal binding (Figure 13).

Figure 12

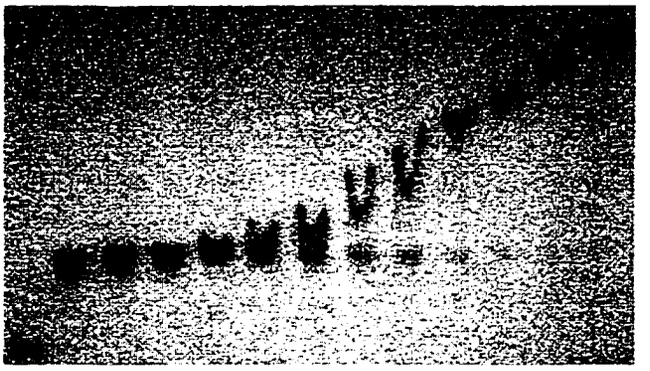

Figure 12. EMSA. Increasing amounts of the GyrA C-terminal domain were incubated with a 300-bp end-labeled DNA fragment for 30 min at 23°C. Reactions were resolved by 4% non-denaturing PAGE. Molar ratio of protein to DNA is indicated.

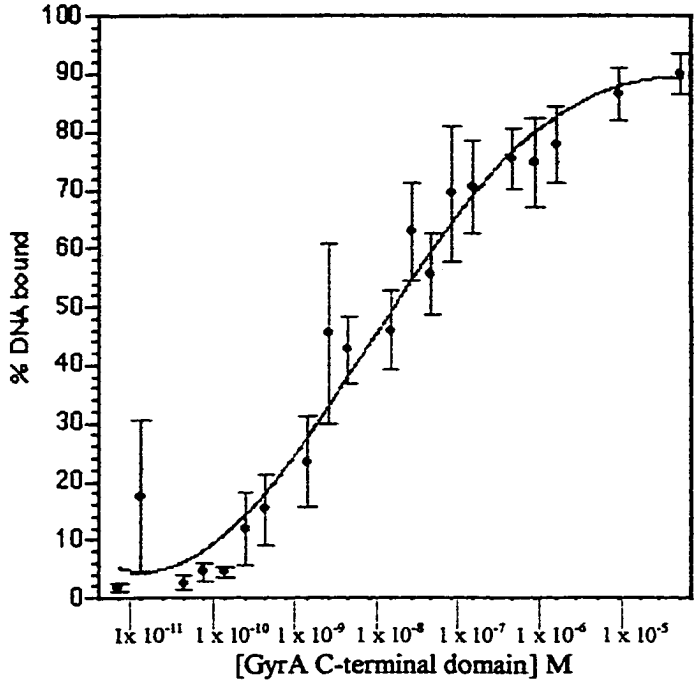

Figure 13. K_d determination. Increasing amounts of the GyrA C-terminal domain were incubated with ~10 pmol of end-labeled DNA for 30 min at 23°C. Reactions were passed through nitrocellulose membranes and the amount of DNA bound to the GyrA C-terminal domain was measured by retention on the membranes. The K_d was determined by the amount of protein required for 50% maximal binding. Data plotted are the mean of five independent experiments. Error bars represent standard error of the mean.

DNA bending activity. The ability of the GyrA C-terminal domain to bend DNA was assayed by T4 DNA ligase-mediated circularization of a 101-bp DNA fragment. In the presence of T4 DNA ligase, the 101-bp DNA fragment containing compatible cohesive ends formed a series of linear multimers (Figure 14A) but did not form circular molecules due to structural rigidity (87). In the presence of the GyrA C-terminal domain, the resulting ligation products consisted primarily of a 101-bp circle, indicating the ability of the protein to bend DNA as small as 101 bp.

To confirm that the main ligation product formed in the presence of the GyrA C-terminal domain was a circular monomer, the ligation product was isolated and digested with various restriction enzymes. The restriction map of the ligation product was compared to the restriction map for the 101-bp linear fragment (Figure 14B and C). Digestion of the linear fragment with *Bfa*I generated a 70-bp labeled fragment and a 30-bp labeled fragment. Similarly, digestion with *Bst*NI resulted in a 80-bp labeled fragment and 20-bp labeled fragment. A double digest using both enzymes yielded 30-bp and 20-bp labeled fragments. Conversely, digestion of the ligation product with either *Bfa*I or *Bst*NI produced a 101-bp linear product, as expected for a 101-bp circular monomer. Digestion of the ligation product with both enzymes yielded a 50-bp labeled fragment, further confirming the ligation product was a circle.

The preference for the GyrA C-terminal domain to bind linear or prebent DNA molecules was analyzed by comparing the affinity of the protein to the 101-bp linear substrate and the 101-bp circular monomer (Figure 15). The GyrA C-terminal domain only bound the linear substrate as assayed by EMSAs, indicating a preference of the

Figure 14

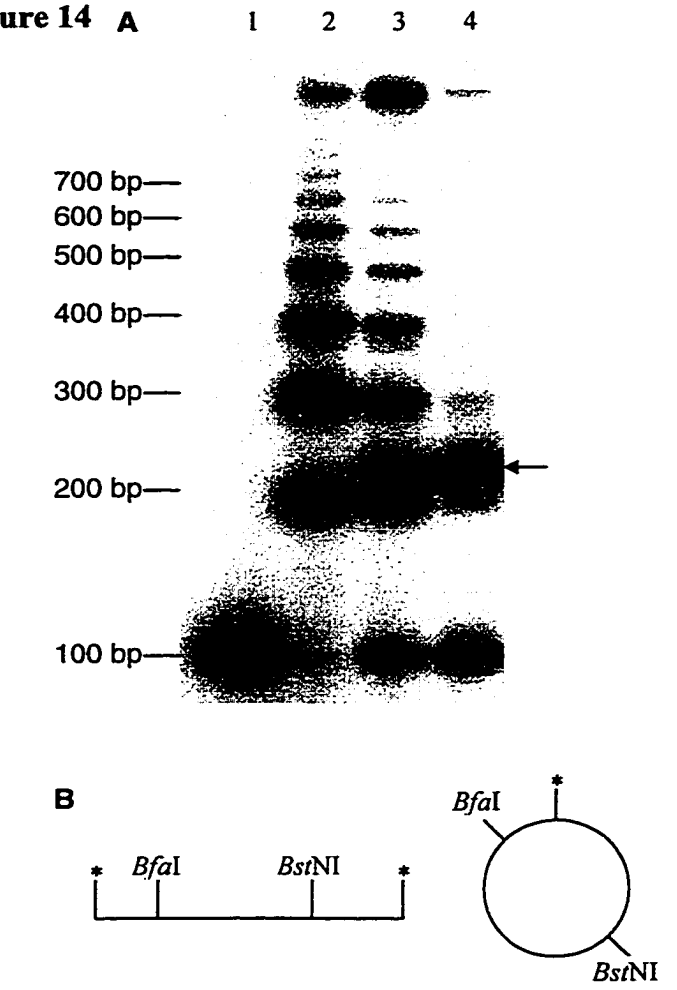

Figure 14. DNA bending. **(A)** Effect of the GyrA C-terminal domain on ligation of 101-bp DNA fragments. DNA (<10 nM) was incubated with T4 DNA ligase in the absence or the presence of the GyrA C-terminal domain. Reactions were resolved by 5% non-denaturing PAGE. Lane 1, 101-bp DNA fragment incubated without ligase; lane 2, 101-bp DNA fragment with ligase; lane 3, 101-bp DNA fragment with 5 nM GyrA C-terminal domain and ligase, lane 4, 101-bp DNA fragment with 10 nM GyrA C-terminal domain and ligase. Sizes of linear multimers are shown in bp, and the arrow indicates the 101-bp circle. **(B)** Diagram of the 101-bp linear and circular DNA molecules. Restriction sites are shown. The * indicates the location of the radioactive label. **(C)** Restriction analysis of the linear and circular DNA molecules. The linear and circular molecules were digested with *Bfa*I, *Bst*NI, or both. Digests were resolved by 12% non-denaturing PAGE. Lanes 1-4, linear 101-bp fragment; Lanes 5- 8, circular 101-bp fragment. Lanes 1 and 5, undigested; lanes 2 and 6 *Bfa*I digest; lanes 3 and 7, *Bst*NI digest; lanes 4 and 8, double digest with *Bfa*I and *Bst*NI. Incomplete digestion in lane 6 resulted in both a linear 101-bp molecule, and an undigested circular 101-bp molecule.

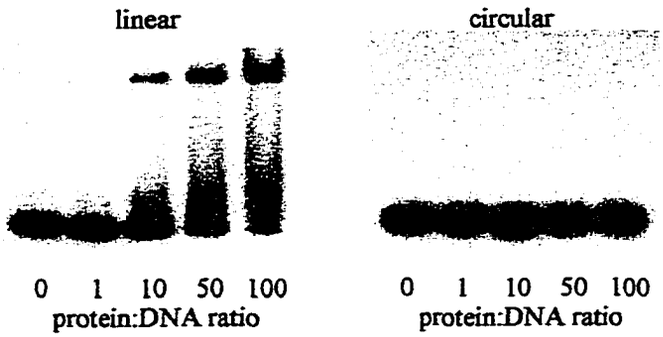

Figure 15. Binding to linear and prebent DNA substrates. Increasing amounts of the GyrA C-terminal domain were incubated with the 101-bp linear or circular substrate, and reactions were resolved by 10% non-denaturing PAGE. The molar ratio of protein to DNA is indicated.

protein to bind linear DNA fragments over prebent fragments by at least 100-fold. Binding to the circular substrate was detected using a 500-fold molar excess of protein (data not shown).

DNA wrapping activity. To determine if the GyrA C-terminal domain was capable of wrapping DNA in addition to bending the helix, we used a DNA ligase-mediated supercoiling assay (72). In the presence of DNA ligase, nicked open-circular DNA molecules formed a mixture of positively and negatively supercoiled topoisomers with a small linking number difference (Figure 16A). With increasing amounts of the GyrA C-terminal domain, the resulting topoisomers became increasingly supercoiled (Figure 16A). This increase was due to toroidal supercoiling: wrapping of the helix around the protein.

Two-dimensional agarose gel electrophoresis was used to determine the direction DNA wraps around the GyrA C-terminal domain (Figure 16B). Wrapping reactions described above were fractionated on agarose gels in the first dimension under native conditions. Electrophoresis in the second dimension was in the presence of non-saturating amounts of chloroquine. Chloroquine is a DNA intercalating agent, which has the effect of unwinding the helix and introducing positive supercoiling to closed circular DNA molecules. At non-saturating amounts of chloroquine, positively supercoiled DNA is accelerated in the second dimension, and negatively supercoiled DNA is retarded in the second dimension. Topoisomers formed by wrapping nicked open-circular DNA with the GyrA C-terminal domain in the presence of DNA ligase were accelerated in the second dimension, indicating that DNA wraps around the protein with positive writhe.

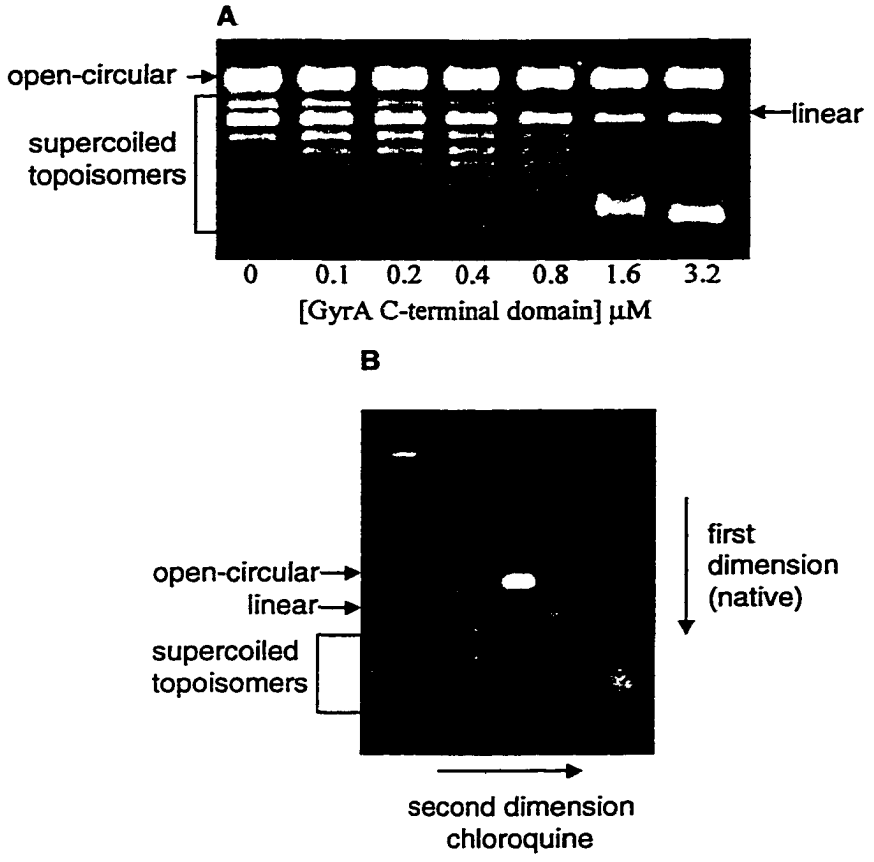

Figure 16. DNA wrapping. (**A**) Toroidal supercoiling. Increasing amounts of the GyrA C-terminal domain were incubated with open-circular DNA. Nicks were sealed by T4 DNA ligase and reactions were resolved on 1% agarose gels. The position of open-circular plasmid, linear plasmid, and supercoiled topoisomers is indicated. (**B**) Two-dimensional agarose gel electrophoresis. DNA supercoiled under conditions described in the 'Materials and Methods' was fractionated on a 1% agarose gel in the first dimension under native conditions. Electrophoresis in the second dimension was in the presence of 1.3 μM chloroquine.

Chapter 6

Genetic disruption of the naturally synthesized *B. burgdorferi* GyrA C-terminal domain

(Adapted from Knight and Samuels, in preparation)

The only selectable marker available to genetically manipulate *B. burgdorferi* is a coumermycin A_1-resistant (cou^r) *gyrB* allele (*gyrB*^{r}) (85, 86). This gene homologously recombines into the chromosome when introduced into *B. burgdorferi* by electroporation (85). Directed insertion of the allele into the circular 26-kb plasmid (cp26) of *B. burgdorferi* has also been accomplished by electroporating DNA fragments containing *gyrB*^{r} flanked with sequences homologous to the target site (76). Using this method, genetic disruption by allelic exchange has been successfully accomplished on cp26 (8, 94, 96).

We disrupted synthesis of the naturally synthesized GyrA C-terminal domain to begin to dissect the function of the protein. Inactivation of the gene by the methods described above for disrupting genes on cp26 was not feasible because it would also disrupt the full-length GyrA product, which is essential in other bacteria and most likely essential in *B. burgdorferi* (84). Instead of insertionally inactivating the gene encoding the GyrA C-terminal domain, we disrupted synthesis of the protein by introducing point mutations that modified the Shine-Dalgarno sequence and changed the first two Met residues of the GyrA C-terminal domain to Leu and Ile residues (Figure 7B). These mutations disrupted synthesis of the GyrA C-terminal domain, while maintaining the GyrA open reading frame. The mutations used to disrupt synthesis of the GyrA C-terminal domain were introduced into *B. burgdorferi* together with mutations in *gyrB* that

conferred resistance to coumermycin A_1. The *gyrB* mutations allowed for selection of recombinants by resistance to coumermycin A_1. A successful recombination event resulted from a crossover and branch migration spanning the cou^r mutations in the 5′ region of *gyrB* and the mutations in the 3′ region of *gyrA* (approximately 4 kb).

Construction of pGACKO. Plasmid pGACKO was constructed using PCR amplification with mutagenic primers. The primers introduced mutations into the Shine-Dalgarno sequence, Met^{499}, and Met^{503} of *gyrA* (Figure 7B and 17). The Met^{499}AUG codon, which is predicted to be the translational start codon, was mutated to a CTT Leu codon to prevent translation of the GyrA C-terminal domain, and the Met^{503} AUG codon was mutated to an ATT Ile codon to prevent translation from initiating downstream. These mutations were made based on the sequence of *E. coli gyrA* and correspond to residues found at the homologous sites in *E. coli* GyrA (93). Silent mutations were also introduced into the Shine-Dalgarno sequence to decrease ribosome binding.

A 4-kb PCR fragment including the 3′ portion of *dnaA*, the complete $gyrB^r$, and the 5′ portion of *gyrA* (basepairs 1-1521) was amplified from B31-NGR. The fragment was amplified using a reverse primer containing the desired mutations. The PCR product was cloned into plasmid pCR.2.1-TOPO to create plasmid pTAKO1 (Figure 18). An 800-bp fragment containing a 3′ fragment of *gyrA* (basepairs 1492-2362) was also PCR-amplified using a mutagenic forward primer and cloned, generating plasmid pTAKO2 (Figure 18). Plasmid pGACKO was created by inserting the ~ 800-bp *Spe*I fragment from plasmid pTAKO2 into the *Spe*I sites in plasmid pTAKO1 (Figure 18). DNA sequencing confirmed insert orientation and the presence of the desired mutations. Plasmid pGACKO was used to transform *B. burgdorferi*.

Figure 17

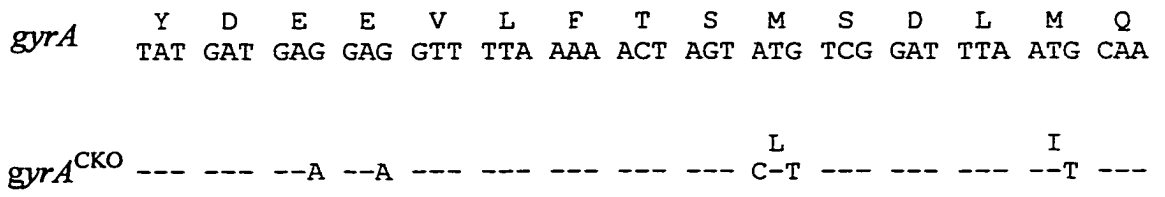

Figure 17. Nucleotide and amino acid sequences of *gyrA* and g*yrA*^{CKO}. Nucleotides 1468-1512 of *gyrA*, which encode amino acids 488-504 of GyrA are shown. Mutations in g*yrA*^{CKO} are indicated along with the corresponding amino acid change. Dashes indicate sequence identity.

Figure 18

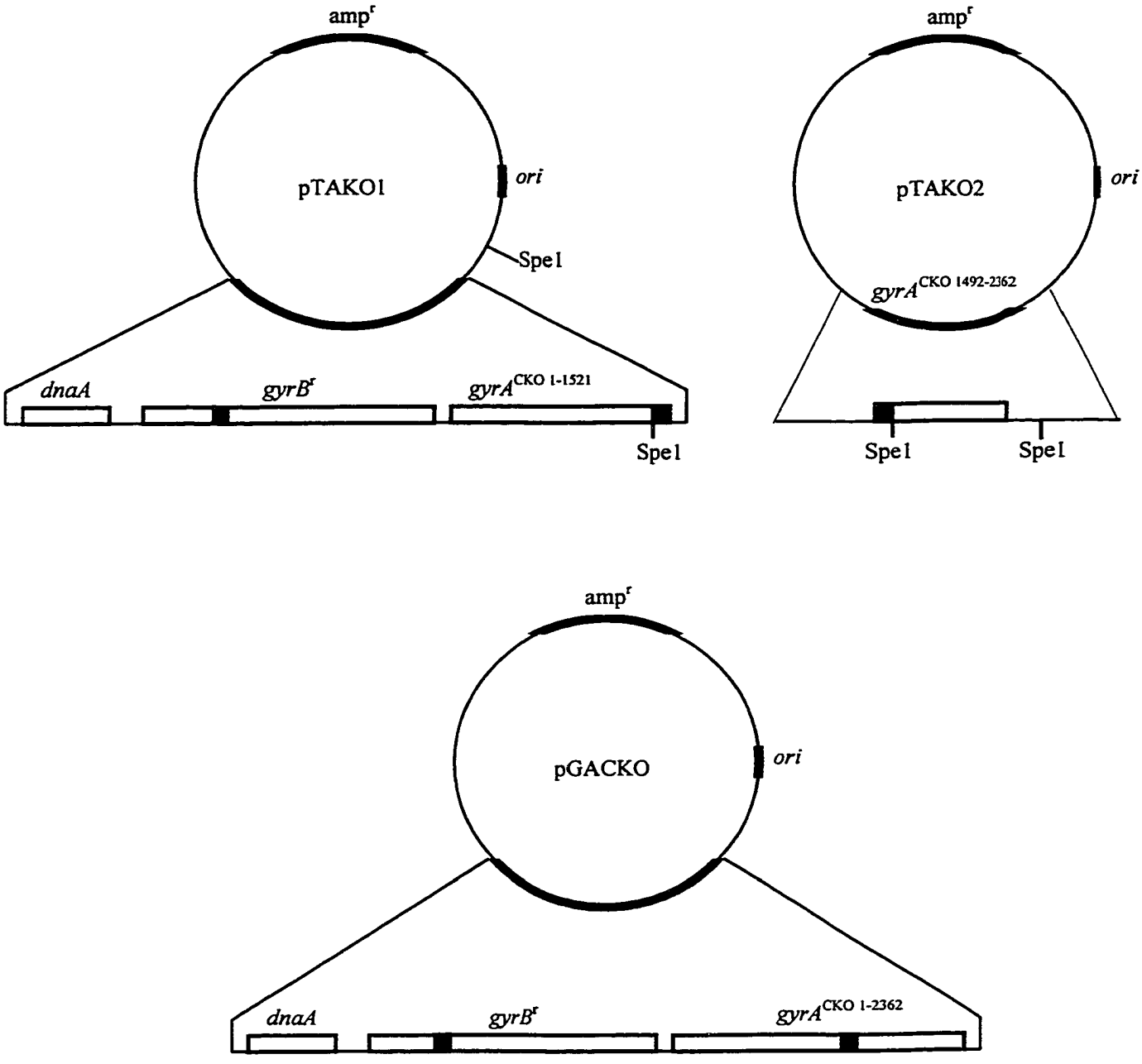

Figure 18. Plasmid constructs. Plasmid pTAKO1 contains the 3′ region of *dnaA*, *gyrB*^{r}, and the first 1521 bp of *gyrA* with the introduced mutations (*gyrA*$^{CKO\ 1\text{-}1521}$). Plasmid pTAKO2 contains basepairs 1492-2362 of *gyrA*^{CKO} (*gyrA*$^{CKO\ 1492\text{-}2362}$). The ~800-bp *Spe*I fragment of plasmid pTAKO2 was cloned into plasmid pTAKO1 at the *Spe*I sites to create plasmid pGACKO. Mutated sites indicated by shaded boxes.

Screening cou^r transformants. *B. burgdorferi* strain B31 was transformed by electroporation with pGACKO and plated in the presence of 0.5 μg ml^{-1} coumermycin A_1. Cou^r transformants were screened for *gyrA* mutations by PCR analysis using primers *gyrA* 1492F/GACKOSC and *gyrA* 2362R. Primer *gyrA* 1492F/GACKOSC is complementary to the mutated sequence in *gyrA*^{CKO}, but only 15 of the 18 nucleotides in the primer are complementary to the wild-type sequence. In addition, a noncomplementary nucleotide is at the 3′ end. These two primers amplify a ~900-bp fragment from *gyrA*^{CKO}, but fail to amplify the same product from wild-type *gyrA* using a 56°C annealing temperature (data not shown).

The results of one screening experiment are shown in Figure 19. Ninety-four transformants were screened by PCR analysis. Two of the 94 colonies yielded a 900-bp PCR product. Three out of 400 (0.7%) coumermycin A_1-resistant colonies screened in this experiment contained the desired mutations as assayed by PCR analysis. The frequency of recombination was approximately twice as efficient as directed insertion of *gyrB*^{r} into cp26 (8, 94, 96). The increase in recombination efficiency over directed insertion into cp26 is possibly due to either the large amount of homologous sequence used for disrupting GyrA C-terminal domain synthesis or the need for only a single crossover, followed by branch migration, rather than a double crossover event. However, because of the large size of the fragment used for recombination, the efficiency remains low. The presence of mutations in positive clones was confirmed by DNA sequencing. Two clones were selected, CKO-1 and CKO-2, for further analysis.

Figure 19

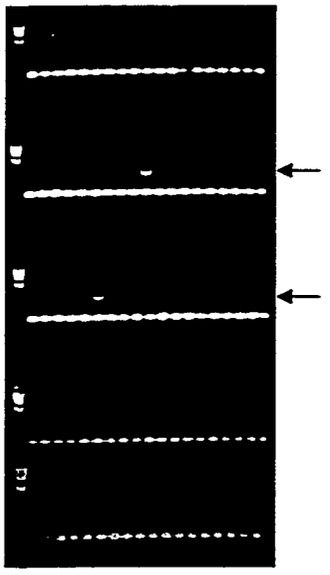

Figure 19. Screening cou^r transformants for *gyrA* mutations. *B. burgdorferi* transformants were PCR-amplified using primers *gyrA* 1492F/GACKOSC and *gyrA* 2362R. Amplification products from 94 colonies were analyzed by agarose gel electrophoresis. A lambda *Hind*III marker was loaded into the first lane of each row. The arrow indicates the position of the 900-bp product. Lower band in each lane is a putative "primer dimer" that is also present in negative controls (data not shown).

Disruption of GyrA C-terminal domain synthesis. Western analysis was used to determine if synthesis of the GyrA C-terminal domain was successfully disrupted (Figure 20). Whole cell lysates from wild-type *B. burgdorferi* strain B31 and CKO-1 were analyzed using the anti-GyrA C-terminal domain antibody. The antibody recognized the full-length GyrA protein in whole cell lysates from CKO-1, but failed to detect the 35-kDa GyrA C-terminal domain, indicating that synthesis of the protein had been successfully disrupted. *B. burgdorferi* strain B31-NGR is isogenic to CKO-1 and CKO-2 with respect to the mutations in *gyrB*. This strain synthesizes the GyrA C-terminal domain at wild-type levels and has an identical protein profile as CKO-1 and CKO-2 as determined by Coomassie stained SDS-PAGE of whole cell lysates (data not shown).

The GyrA C-terminal domain is not essential for growth *in vitro*. We have hypothesized that the GyrA C-terminal domain functions in linear DNA metabolism in *B. burgdorferi*. To test this hypothesis, we used a variety of assays to determine a phenotype of the GyrA C-terminal domain-deficient strains of *B. burgdorferi*, focusing on linear DNA structure and gene expression. The linear plasmids were maintained in CKO-1 and CKO-2 as examined by ethidium bromide staining of DNA extracts fractionated by agarose gel electrophoresis (data not shown). We also examined the nucleoid morphology in strains CKO-1 and CKO-2 by 4′, 6-diamidino-2-phenylindole (DAPI) staining. Using this method, there were no detectable differences in gross DNA structure or morphology in strains CKO-1 or CKO-2 compared to either strain B31 or the isogenic strain B31-NGR (data not shown). No differences in gene expression of the GyrA C-

Figure 20

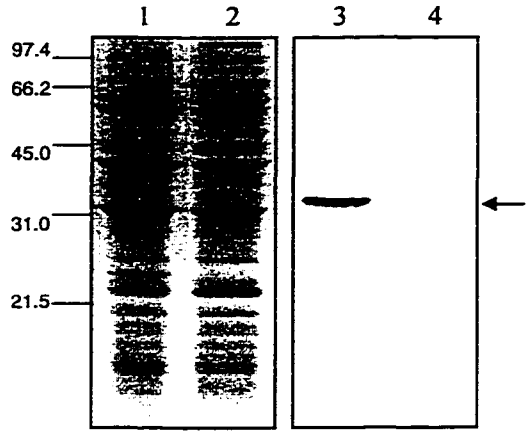

Figure 20. Western analysis. Whole cell *B. burgdorferi* lysates were resolved by 12.5% SDS-PAGE. Lanes 1 and 3, strain B31; lanes 2 and 4, strain CKO. Lanes 1 and 2 were stained with Coomassie brilliant blue. Lanes 3 and 4 were Western blotted and probed with anti-GyrA C-terminal domain polyclonal antiserum. Arrow indicates the location of the GyrA C-terminal domain. Molecular mass standards shown in kilodaltons.

terminal domain-deficient strains compared to strain B31-NGR were detected by Coomassie-stained SDS-PAGE gels of whole cell lysates (data not shown). *gyrA* expression and *hbb* expression also remained unchanged as determined by Western analyses (data not shown). The GyrA C-terminal domain-deficient strains grow in both liquid culture and semi-solid medium, and they exhibit a similar morphology to and growth rate as B31 and B31-NGR (data not shown).

Chapter 7

DISCUSSION

7.1 Synthesis of the GyrA C-terminal domain.

The GyrA C-terminal domain in *B. burgdorferi* is the first example of a bacterium naturally synthesizing a domain of DNA gyrase as a separate protein, distinct from the subunits found in the holoenzyme. The synthesis of the GyrA C-terminal domain is controlled by an expression system rarely found in a prokaryotic cellular genome: a smaller protein encoded on a separate transcript that is initiated within a full-length gene and translated in the identical reading frame as a larger protein. In *B. burgdorferi*, translation of the GyrA C-terminal domain is initiated at Met^{499} of GyrA, and transcription of the 1200-nt mRNA encoding the protein is initiated from three separate start sites located within *gyrA*. The three start sites may be a means to regulate expression of the gene encoding the 35-kDa protein by using different start sites under different conditions. Based on the Northern and primer extension data, we predict that nts 1430 and 1435, which are separated by one turn of the helix, are the two predominant start sites.

Expression of the gene encoding the 35-kDa protein may be complex considering the promoter for the gene is located within *gyrA*, which is expressed at an approximately four-fold lower level than the gene encoding the GyrA C-terminal domain. Adding to the complexity associated with transcription being initiated within another gene is the possibility that translation of the 35-kDa protein may be initiated from both the 1200-nt transcript and the larger 5000-nt bicistronic message.

7.2 HU-like activity of the GyrA C-terminal domain.

As unexpected as the synthesis of this unique protein is the ability of the GyrA C-terminal domain to substitute for HU *in vitro* and complement an HU deficient mutant of *E. coli in vivo*. Initial stages of Mu transposition both *in vitro* and *in vivo* require HU (18, 39). The formation of the Type 1 complex necessitates the assembly of a multi-protein complex consisting of Mu A, HU, and IHF on a supercoiled donor molecule (15). We demonstrate here that the GyrA C-terminal domain from *B. burgdorferi* substitutes for HU in forming the Type 1 complex in Mu transposition. The eukaryotic protein HMG1 will also substitute efficiently for HU in this reaction (46). HU and HMG1, although from different domains of life, share similar activities both *in vitro* and *in vivo* (4). The efficient substitution of the *B. burgdorferi* GyrA C-terminal domain for HU in the Mu donor-cleavage reaction indicates a specific HU-like activity for the protein found only in the functionally related proteins HU and HMG1.

In *E. coli*, a 33-kDa protein consisting of the GyrA C-terminal domain can be generated by proteolytic cleavage of GyrA or by expression of a recombinant gene product (72, 74). The naturally occurring protein from *B. burgdorferi* and the homologous region from the *E. coli* GyrA are biochemically distinct, sharing only 24% identity at the amino acid level. The GyrA C-terminal domain from *E. coli* is acidic with a predicted isoelectric point (pI) of 4.0; in contrast, the naturally occurring 35-kDa protein from *B. burgdorferi* is basic with a predicted pI of 9.1. Like the GyrA C-terminal domain of *B. burgdorferi*, the 33-kDa protein from *E. coli* binds DNA nonspecifically, with multiple protein molecules binding each DNA molecule (72). Both the recombinant *E. coli* 33-kDa protein and the *B. burgdorferi* 35-kDa protein wrap DNA with positive

writhe (72). Despite these similar DNA-binding activities, the recombinant 33-kDa GyrA C-terminal domain from *E. coli* was not capable of substituting for HU under standard reaction conditions in the *in vitro* Mu donor-cleavage reaction (data not shown), indicating that the *B. burgdorferi* GyrA C-terminal domain possesses a unique HU-like function that is not merely a consequence of binding DNA nonspecifically and altering the writhe.

The GyrA C-terminal domain not only forms higher-order nucleoprotein complexes *in vitro*, but the gene encoding the GyrA C-terminal domain complements an *E. coli hupA hupB* mutant as measured by bacteriophage Mu growth. This indicates that the protein also functions in forming these assemblies *in vivo*. The previously identified gene encoding the HU/IHF homolog in *B. burgdorferi*, *hbb*, is incapable of complementing the defect in Mu growth found in *hupA hupB E. coli* strains (95). However, *hbb* complements an HU/IHF deficient mutant as assayed by restoring a bacteriophage lambda packaging defect (95). Whereas bacteriophage lambda growth requires either HU or IHF, Mu growth has a strict requirement for HU (39, 59). The previously identified HU/IHF homolog, Hbb, may be synthesized at much lower levels than the GyrA C-terminal domain, since extensive attempts to purify Hbb from *B. burgdorferi* have been unsuccessful (95). In addition, immunoblot analyses with an antibody against a synthetic peptide reveal little Hbb protein in cell lysates (42). We report here that the GyrA C-terminal domain is an abundant nonspecific DNA-binding protein in *B. burgdorferi*, with an activity and a cellular concentration similar to HU. Taken together, these data suggest that Hbb may function more similarly to IHF in *B. burgdorferi*, while the GyrA C-terminal domain provides an HU-like function. In

support of this, preliminary data suggest that Hbb can bind DNA with sequence specificity (42).

The GyrA C-terminal domain has not been identified as a naturally synthesized HU-like protein in any other prokaryote outside of the *Borrelia*. However, the activities of DNA gyrase and HU are linked. HU stimulates DNA gyrase decatenation activity *in vitro* and HU suppressor mutations have been mapped to *gyrB* (51, 56). DNA gyrase and HU alter the superhelical path of the DNA helix using different mechanisms. DNA gyrase affects DNA topology by changing the linking number, and HU affects DNA writhe by bending or wrapping the helix. *Borrelia* has apparently been able to more intimately join the supercoiling and bending activities of these two proteins by synthesizing the DNA gyrase domain responsible for wrapping DNA as a separate HU-like protein. We speculate that this unique protein evolved as an adaptation for the presence of linear hairpin-containing replicons. Alternatively, the unique expression of this HU-like protein from *gyrA* may be a means for *Borrelia* to compensate for its small genome size of approximately 1.2 Mb by expressing domains of larger proteins as distinct functional products.

7.3 DNA-binding activity.

Initial studies demonstrated that the naturally synthesized GyrA C-terminal domain from *B. burgdorferi* binds DNA non-specifically, with multiple protein molecules binding each DNA molecule. These experiments were performed in the presence of the nonspecific competitor poly-dIdC. Because the GyrA C-terminal domain binds DNA nonspecifically, we examined the binding of the protein to a 300-bp substrate in the absence of competitor DNA. The protein formed a distinct complex with DNA at an

equal molar ratio of protein to DNA up to an approximately 16-fold excess of protein. Evidence of multiple protein molecules binding to each DNA molecule was observed only above a 16-fold molar excess of protein to DNA. The structure of the larger protein-DNA complexes formed in the excess of the GyrA C-terminal domain is unknown. The continuing decrease in mobility of these complexes suggests that multiple protein molecules are binding each DNA molecule; at high concentrations of the GyrA C-terminal domain, the protein may be coating the DNA molecule.

Protein-protein interactions may also be involved in forming the supershifted complexes observed at high protein concentrations. The GyrA C-terminal domain is a monomer in solution, in contrast to the functionally related HU protein, which, like many other small-DNA binding proteins, is a dimer in solution. Binding of the GyrA C-terminal domain to DNA may require the formation of a protein dimer, or protein-protein interactions may only form at high protein concentrations. Protein-protein contacts are necessary in forming a functional DNA gyrase enzyme, with GyrA and GyrB protomers interacting with identical subunits and each other in the heterotetramer (73). Protein-protein interactions involving GyrA have been identified in the N-terminal domain of the protein, but no protein-protein interactions have been mapped to the C-terminal domain of the protein (73). Contacts in the C-terminal domain of GyrA may be important in the holoenzyme during different stages of the supercoiling activity, but lack of structural data in this area of the enzyme has limited such investigations.

The GyrA C-terminal domain has a higher affinity for DNA than the functionally related *E. coli* HU protein ($K_d = 1.3 \times 10^{-5}$ M) (7). Conversely, the GyrA C-terminal domain has a weaker affinity for DNA than *E. coli* DNA gyrase ($K_d = 1 \times 10^{-10}$ to

5 x 10^{-10}M) (35, 58). The difference in affinity for DNA between the *B. burgdorferi* GyrA C-terminal domain and *E. coli* DNA gyrase is likely due to the multiple contacts DNA gyrase makes with the helix in addition to the contacts made in the GyrA C-terminal domain (73). The differences in binding affinity between the *B. burgdorferi* GyrA C-terminal domain, *E. coli* HU, and *E. coli* DNA gyrase may be partially attributed to differences in substrates and assays used in determining dissociation constants for the different proteins (7, 35).

The GyrA C-terminal domain bends DNA upon binding and wraps DNA at higher protein concentrations. The observed wrapping activity of the protein is likely a result of multiple protein molecules binding to the open-circular substrate, each inducing a bend that collectively introduces toroidal supercoiling into the DNA molecule. A similar mechanism of toroidal supercoiling has been attributed to the 33-kDa C-terminal domain of GyrA from *E. coli*, which wraps DNA with each protein molecule contributing 1/40 of a positive turn (72).

The bending and wrapping activities of the GyrA C-terminal domain is similar to the activity of the *E. coli* HU protein. Both HU and the GyrA C-terminal domain bend DNA and constrain supercoils (11, 37). However, the direction DNA wraps around the two proteins is opposite. HU constrains negative supercoils, and the GyrA C-terminal domain constrains positive supercoils (11). Based on the opposite wrapping activities of HU and the GyrA C-terminal domain, substitution of the *B. burgdorferi* GyrA C-terminal domain for HU in the Mu donor cleavage reaction, which consists of a series of ordered protein-DNA and protein-protein interactions, is somewhat surprising (15).

The GyrA C-terminal domain readily binds to linear DNA molecules, but the protein does not bind to prebent molecules with high affinity. In contrast, HU prefers binding prebent molecules (7). The bending activity of the GyrA C-terminal domain coupled with the preference for binding linear DNA molecules over prebent molecules, suggests a possible model for the binding observed with the 300-bp linear DNA fragment. The conformational change induced by binding of one molecule of the GyrA C-terminal domain may distort the entire 300-bp fragment. The helix may be deformed to such an extent that an additional protein molecule will not bind again until high protein concentrations are reached, as is observed for the prebent 101-bp circular molecule.

The *B. burgdorferi* genome is approximately 1 Mb, with each cell containing 8-16 copies of the genome. Approximately 30,000 GyrA C-terminal domain molecules are present in each cell. Assuming 8 copies of the genome are in each cell, and that the GyrA C-terminal domain is distributed uniformly throughout the genome, then there would be approximately one protein dimer per 500 bp of DNA. This is nearly identical to the HU distribution in *E. coli*, with approximately one HU dimer per 500 bp of DNA (103).

Although the cellular function of the GyrA C-terminal domain in *B. burgdorferi* is unknown, the results described previously and the findings reported here suggests a possible role for this unique protein. The distortion of the helix upon binding of the GyrA C-terminal domain may regulate DNA topology by toroidal supercoiling and is suggestive of a structural role in DNA packaging. Likewise, DNA deformation induced by GyrA C-terminal domain binding may be mechanistically involved in a variety of DNA transactions. The interaction of the GyrA C-terminal domain with DNA is similar to the interaction of HU with DNA, but there are notable differences. These may be due

to differences in the structural requirements for the predominantly linear genome found in *B. burgdorferi* and the circular genome of *E. coli*.

7.4 Disruption of the synthesis of the GyrA C-terminal domain.

To begin to understand the role of the GyrA C-terminal domain in *B. burgdorferi*, we disrupted synthesis of the protein by mutating nucleotides critical for its translation. These mutations were linked to the *gyrB*^{r} allele, allowing for selection of transformants by coumermycin A_1 resistance. Although synthesis of the GyrA C-terminal domain was disrupted, the GyrA open reading frame was maintained. This is the first example of inactivating a *B. burgdorferi* gene by the introduction of specific point mutations.

The ability to disrupt synthesis of the GyrA C-terminal domain clearly demonstrates that this protein is nonessential. Based on our demonstration of the HU-like activity of the protein, this finding is not surprising. *E. coli* strains lacking both subunits of HU are viable, with no dramatic defects in macromolecular metabolism (63). Major abnormalities of these *E. coli* strains include slow doubling times, a deficiency in plasmid maintenance, and the inability to support bacteriophage Mu growth (39, 66, 99). Some of the observed phenotypes are unstable and are compensated by the accumulation of suppressor mutations (39). Interestingly, suppressor mutations have been mapped to *gyrB*, which encodes the other DNA gyrase subunit, suggesting a possible interplay between DNA gyrase and HU (51).

We have not yet identified a distinct phenotype for the *B. burgdorferi* strain lacking the GyrA C-terminal domain. *E. coli* HU has little effect on transcriptional promoter regulation other than its own (39, 43), and the *B. burgdorferi* GyrA C-terminal domain may likewise have little effect on regulating gene expression. We are currently

examining the effects the GyrA C-terminal domain has on regulating its own promoter in the deficient strain. These studies may indicate a functional role for this unique protein. In addition, we are analyzing the maintenance of circular plasmids in the GyrA C-terminal domain deficient strains.

7.5 Possible function of the GyrA C-terminal domain.

Most . [c]our understanding of the possible *in vivo* role of this protein comes from experiments performed in *E. coli* and comparisons to the functionally related *E. coli* HU protein. We speculate that the GyrA C-terminal domain participates in a variety of reactions by promoting the formation of nucleoprotein complexes. The protein is clearly nonessential, at least in culture, so its function, although not critical, may be to simply facilitate a number of DNA transactions.

The HU-like activity of the GyrA C-terminal domain, especially in its role in promoting recombination intermediates, raises the question of whether the protein functions in similar recombination systems in *B. burgdorferi.* Recombination occurs in *B. burgdorferi* (77, 85) and an elaborate system exists for antigenic variation (104). The ability of the GyrA C-terminal domain to support recombination in the Mu system suggests that the protein may have a similar role in *B. burgdorferi* recombination. If so, involvement in antigenic variation may have important implications for pathogenesis. Numerous copies of a putative recombinase/transposase resembling an IS891-like transposase is found throughout the plasmid sequences, and a bacteriophage has been identified (23, 26). Parallels to the Mu system and the HU-like activity of the GyrA C-terminal domain again suggest that the protein may be involved in the metabolism of these genetic elements. The function of the GyrA C-terminal domain *B. burgdorferi* will

likely continue to unfold as a genetic system to manipulate the organism is further developed.

Chapter 8

References

1. **Barbour, A. G., C. J. Carter, V. Bundoc, and J. Hinnebusch.** 1996. The nucleotide sequence of a linear plasmid of *Borrelia burgdorferi* reveals similarities to those of circular plasmids of other prokaryotes. J. Bacteriol. **178:**6635-6639.
2. **Barbour, A. G., and C. F. Garon.** 1987. Linear plasmids of the bacterium *Borrelia burgdorferi* have covalently closed ends. Science. **237:**409-411.
3. **Bates, A. D., and A. Maxwell.** 1993. DNA topology. Oxford University Press, Oxford, England.
4. **Bianchi, M. E.** 1994. Prokaryotic HU and eukaryotic HMG1: a kinked relationship. Mol. Microbiol. **14:**1-5.
5. **Blackburn, E. H.** 1991. Structure and function of telomeres. Nature. **350:**569-573.
6. **Boles, T. C., J. H. White, and N. R. Cozzarelli.** 1990. Structure of plectonemically supercoiled DNA. J. Mol. Biol. **213:** 931-951.
7. **Bonnefoy, E., M. Takahashi, and J. Rouviere-Yaniv.** 1994. DNA-binding parameters of the HU protein of *Escherichia coli* to cruciform DNA. J Mol Biol. **242:**116-129.
8. **Bono, J. L., K. Tilly, B. Stevenson, D. Hogan, and P. Rosa.** 1998. Oligopeptide permease in *Borrelia burgdorferi*: putative peptide-binding components encoded by both chromosomal and plasmid loci. Microbiology. **144:**1033-1044.
9. **Bramhill, D., and A. Kornberg.** 1988. Duplex opening by dnaA protein at novel sequences in initiation of replication at the origin of the *E. coli* chromosome. Cell. **52:**743-755.
10. **Brown, T.** 1996. *In* F. M. Ausubel, R. Brent, R. E. Kingston, D. D. Moore, J. G. Seidman, J. A. Smith, and K. Struhl (ed.), Current Protocols in Molecular Biology, John Wiley and Sons, CD-ROM, unit 4.9.
11. **Broyles, S. S., and D. E. Pettijohn.** 1986. Interaction of the *Escherichia coli* HU protein with DNA: evidence for formation of nucleosome-like structures with altered DNA helical pitch. J. Mol. Biol. **187:**47-60.
12. **Bukhari, A. I., and E. Ljungquist.** 1977. Bacteriophage Mu: methods for cultivation and use, p. 749-756. *In* A. I. Bukhari, J. A. Shapiro, and S. L. Adhya (ed.), DNA insertion elements, plasmids, and episomes. Cold Spring Harbor Laboratory, Cold Spring Harbor, N. Y.
13. **Busby, S., A. Kolb, and H. Buc.** 1979. Isolation of plasmid-protein complexes from *Escherichia coli*. Eur. J. Biochem. **99:**105-111.
14. **Casjens, S., R. v. Vugt, B. Stevenson, K. Tilly, and P. Rosa.** 1997. Homology throughout the multiple 32-kilobase circular plasmids present in Lyme disease spirochetes. J. Bacteriol. **17:**217-227.
15. **Chaconas, G., B. D. Lavoie, and M. A. Watson.** 1996. DNA transposition: jumping gene machine, some assembly required. Curr. Biol. **6**(7)**:**817-820.
16. **Chang, P. C., and S. N. Cohen.** 1994. Bidirectional replication from an internal origin in a linear *Streptomyces* plasmid. Science. **265:**952-957.

17. **Cozzarelli, N. R.** 1980. DNA gyrase and the supercoiling of DNA. Science. **207:**953-960.
18. **Craigie, R., D. J. Arndt-Jovin, and K. Mizuuchi.** 1985. A defined system for the DNA strand-transfer reaction at the initiation of bacteriophage Mu transposition: protein and DNA substrate requirements. Proc. Natl. Acad. Sci. USA. **82:**7570-7574.
19. **Ditto, M. D., D. Roberts, and R. A. Weisberg.** 1994. Growth phase variation of integration host factor level in *Escherichia coli.* J. Bacteriol. **176**(12):3738-3748.
20. **Drlica, K., and J. Rouviere-Yaniv.** 1987. Histonelike proteins of bacteria. Microbiol. Rev. **51:**301-319.
21. **Echols, H.** 1986. Multiple DNA-protein interactions governing high-precision DNA transactions. Science. **233:**1050-1056.
22. **Echols, H.** 1990. Nucleoprotein structures initiating DNA replication, transcription, and site-specific recombination. J. Biol. Chem. **265**(25):14697-14700.
23. **Eggers, C. H., and D. S. Samuels.** unpublished data.
24. **Ferdows, M. S., P. Serwer, G. A. Griess, S. J. Norris, and A. G. Barbour.** 1996. Conversion of a linear to a circular plasmid in the relapsing fever agent *Borrelia hermsii.* J. Bacteriol. **178:** 793-800.
25. **Fraser, C. M., *et al.*** 1998. Complete genome sequence of *Treponema pallidum*, the syphilis spirochete. Science. **281:**375-388.
26. **Fraser, C. M., *et al.*** 1997. Genomic sequence of a Lyme disease spirochaete, *Borrelia burgdorferi.* Nature. **390:**580-586.
27. **Fraser, C. M., *et al.*.** 1995. The minimal gene complement of *Mycoplasma genitalium.* Science. **270:**397-403.
28. **Fuller, R. S., and A. Kornberg.** 1983. Purified dnaA protein in initiation of replication at the *Escherichia coli* chromosomal origin of replication. Proc. Natl. Acad. Sci. USA. **80:**5817-5821.
29. **Gardner, J. F., and H. A. Nash.** 1986. Role of *Escherichia coli* IHF protein in lambda site-specific recombination: a mutational analysis of binding sites. J. Mol. Biol. **191:**181-189.
30. **Gellert, M., K. Mizuuchi, M. H. O'Dea, and H. A. Nash.** 1976. DNA gyrase: an enzyme that introduces superhelical turns into DNA. Proc. Natl. Acad. Sci. USA. **73:**3872-3876.
31. **Griffith, J. D.** 1976. Visualization of prokaryotic DNA in a regulatory condensed chromatin-like fiber. Proc. Natl. Acad. Sci. USA. **73:**563-567.
32. **Hagerman, P. J.** 1990. Sequence-directed curvature of DNA. Annu. Rev. Biochem. **59:**755-81.
33. **Hayakawa, T., T. Tanaka, K. Sakaguchi, N. Otake, and H. Yonehara.** 1979. A linear plasmid-like DNA in *Streptomyces* species producing lankacidin group antibiotics. J. Gen. Appl. Microbiol. **25:**255-260.
34. **Hayes, J. J., D. J. Clark, and A. P. Wolffe.** 1991. Histone contributions to the structure of DNA in the nucleosome. Proc. Natl. Acad. Sci. USA. **88:**6829-6833.
35. **Higgins, N. P., and N. R. Cozzarelli.** 1982. The binding of gyrase to DNA: analysis by retention by nitrocellulose filters. Nucleic Acids Res. **10**(21):6833-6846.

36. **Hinnebusch, J., and K. Tilly.** 1993. Linear plasmids and chromosomes in bacteria. Mol. Microbiol. **10**(5):917-922.
37. **Hodges-Garcia, Y., P. J. Hagerman, and D. E. Pettijohn.** 1989. DNA ring closure mediated by protein HU. J. Biol. Chem. **264**(25):14621-14623.
38. **Huang, W. M.** 1992. Multiple DNA gyrase-like genes in eubacteria, p. 39-48. *In* T. Andoh, H. Ikeda, and M. Oguro (ed.), Molecular biology of DNA topoisomerases and its application to chemotherapy. CRC Press, Boca Raton, Florida.
39. **Huisman, O., M. Faelen, D. Girard, A. Jaffe, A. Toussaint, and J. Rouviere-Yaniv.** 1989. Multiple defects in *Escherichia coli* mutant lacking HU protein. J. Bacteriol. **171**:3704-3712.
40. **Kampranis, S. C., and A. Maxwell.** 1996. Conversion of DNA gyrase into a conventional type II topoisomerase. Proc. Natl. Acad. Sci. USA. **93**:14416-14421.
41. **King, C. Y., and M. A. Weiss.** 1993. The SRY high-mobility-group box recognizes DNA by partial intercalation in the minor groove: a topological mechanism of sequence specificity. Proc. Natl. Acad. Sci. USA. **90**:11990-11994.
42. **Knight, S. W., C. Schwanke, and D. S. Samuels.** unpublished data.
43. **Kohno, K., M. Wada, Y. Kano, and F. Imamoto.** 1990. Promoters and autogenous control of the *Escherichia coli hupA* and *hupB* genes. J. Mol. Biol. **213**:27-36.
44. **Kornberg, A., and T. A. Baker.** 1992. DNA Replication, 2 ed. W. H. Freeman and Company, New York, NY.
45. **Kremer, W., K. Klenin, S. Diekmann, and J. Langowski.** 1993. DNA curvature influences the internal motions of supercoiled DNA. EMBO J. **12**:4407-4412.
46. **Lavoie, B. D., and G. Chaconas.** 1994. A second high affinity HU binding site in the phage MU transpososome. J. Biol. Chem. **269**(22):15571-15576.
47. **Lavoie, B. D., and G. Chaconas.** 1993. Site-specific HU binding in the Mu transposome: conversion of a sequence-independent DNA-binding protein into a chemical nuclease. Genes & Development. **7**:2510-2519.
48. **Lavoie, B. D., G. S. Shaw, A. Millner, and G. Chaconas.** 1996. Anatomy of a flexer-DNA complex inside a higher-order transposition intermediate. Cell. **85**:761-771.
49. **Liu, L. F., and J. C. Wang.** 1978. DNA-DNA gyrase complex: the wrapping of the DNA duplex outside the enzyme. Cell. **15**:979-984.
50. **Liu, L. F., and J. C. Wang.** 1987. Supercoiling of the DNA template during transcription. Proc. Natl. Acad. Sci. USA. **84**:7024-7027.
51. **Malik, M., A. Bensaid, J. Rouviere-Yaniv, and K. Drlica.** 1996. Histone-like protein HU and bacterial DNA topology: suppression of an HU deficiency by gyrase mutations. J. Mol. Biol. **256**:66-76.
52. **Marconi, R. T., S. Casjens, U. G. Munderloh, and D. S. Samuels.** 1996. Analysis of linear plasmid dimers in *Borrelia burgdorferi* sensu lato isolates: implications concerning the potential mechanism of linear plasmid replication. J Bacteriol. **178**(11):3357-61.

53. **Marconi, R. T., D. S. Samuels, and C. F. Garon.** 1993. Transcriptional analysis and mapping of the *osp*C gene in Lyme disease spirochetes. J. Bacteriol. **175**(4):926-932.
54. **Margolis, N., D. Hogan, K. Tilly, and P. A. Rosa.** 1994. Plasmid location of *Borrelia* purine biosynthesis gene homologs. J. Bacteriol. **176:**6427-6432.
55. **Margolis, N., and D. S. Samuels.** 1995. Proteins binding to the promoter region of the operon encoding the major outer surface proteins OspA and OspB of *Borrelia burgdorferi.* Mol. Biol. Rep. **21**(3):159-64.
56. **Marians, K. J.** 1987. DNA gyrase-catalyzed decatenation of multiply linked DNA dimers. J. Biol. Chem. **262**(21):10362-10368.
57. **Materman, E., and A. v. Gool.** 1978. Compact *Escherichia coli* nucleoids in a highly supercoiled conformation. J. Bacteriol. **135:**703-706.
58. **Maxwell, A., and M. Gellert.** 1984. The DNA dependence of the ATPase activity of DNA gyrase. J. B. C. **259:**14472.
59. **Mendelson, I., M. Gottesman, and A. B. Oppenheim.** 1991. HU and integration host factor function as auxiliary proteins in cleavage of phage lambda cohesive ends by terminase. J. Bacteriol. **163:**787-791.
60. **Menzel, R., and M. Gellert.** 1987. Fusions of the *Escherichia coli gyrA* and *gyrB* control regions to the galactokinase gene are inducible by coumermycin treatment. J. Bacteriol. **169:**1272-1278.
61. **Micka, B., N. Grouch, U. Heinemann, and M. A. Marahiel.** 1991. Molecular cloning, nucleotide sequence, and characterization of the *Bacillus subtilis* gene encoding the DNA-binding protein HBsu. J. Bacteriol. **173:**3191-3198.
62. **Naigamwalla, D. Z., and G. Chaconas.** 1997. A new set of Mu DNA transposition intermediates: alternate pathways of target capture preceding strand transfer. EMBO J. **16**(17):5227-5234.
63. **Nash, H. A.** 1996. The HU and IHF proteins: accessory factors for complex protein-DNA assemblies, p. 149-179. *In* E. C. C. Lin and A. S. Lynch (ed.), Regulation of Gene Expression. R. G. Landes Company, Austin, Texas.
64. **Nash, H. A., K. Mizuuchi, and R. A. Weisberg.** 1977. Integrative recombination of bacteriophage lambda-the biochemical approach to DNA insertion, p. 363-373. *In* A. I. Bukhari, J. A. Shapiro, and S. L. Adhya (ed.), DNA insertion elements, plasmids, and episomes. Cold Spring Harbor Press, Cold Spring Harbor.
65. **Ner, S. S., and A. A. Travers.** 1994. Harnessing the writhe: a role for DNA chaperones in nucleoprotein-complex formation. Trends Biochem. Sci. **19**(5):185-187.
66. **Ogura, T., H. Niki, Y. Kano, F. Imamoto, and S. Hiraga.** 1990. Maintenance of plasmids in HU and IHF mutants of *Escherichia coli.* Mol Gen Genet. **220:**197-203.
67. **Otwinowski, Z., R., *et al.*** 1988. Crystal structure of *trp* repressor/operator complex at atomic resolution. Nature. **355:**321-329.
68. **Perez-Martin, J., and V. d. Lorenzo.** 1997. Clues and consequences of DNA bending in transcription. Annu. Rev. Microbiol. **51:**593-628.
69. **Pettijohn, D. E.** 1988. Histone-like proteins and bacterial chromosome structure. J. Biol. Chem. **263**(26):12793-12796.

70. **Picardeau, M., J. R. Lobry, and B. J. Hinnebusch.** 1999. Physical mapping of an origin of bidirectional replication at the centre of the *Borrelia burgdorferi* linear chromosome. Mol. Microbiol. **32**:437-445.

71. **Pil, P. M., C. S. Chow, and S. J. Lippard.** 1993. High-mobility-group 1 protein mediates DNA bending as determined by ring closures. Proc. Natl. Acad. Sci. USA. **90**:9465-9469.

72. **Reece, R. J., and A. Maxwell.** 1991. The C-terminal domain of the *Escherichia coli* DNA gyrase A subunit is a DNA-binding protein. Nucleic Acids Res. **19**(7):1399-1405.

73. **Reece, R. J., and A. Maxwell.** 1991. DNA gyrase: structure and function. Crit. Rev. Biochem. Mol. Biol. **26**(3/4):335-375.

74. **Reece, R. J., and A. Maxwell.** 1989. Tryptic fragments of the *Escherichia coli* DNA gyrase A protein. J. Biol. Chem. **264**(33):19648-19653.

75. **Roca, J., J. M. Berger, S. C. Harrison, and J. C. Wang.** 1996. DNA transport by a type II topoisomerase: direct evidence for a two-gate mechanism. Proc. Natl. Acad. Sci. USA. **93**:4057-4062.

76. **Rosa, P., D. S. Samuels, D. Hogan, B. Stevenson, S. Casjens, and K. Tilly.** 1996. Directed insertion of a selectable marker into a circular plasmid of *Borrelia burgdorferi*. J Bacteriol. **178**(20):5946-53.

77. **Rosa, P. A., T. Schwan, and D. Hogan.** 1992. Recombination between genes encoding major outer surface proteins A and B of *Borrelia burgdorferi*. Mol. Microbiol. **6**:3031-3040.

78. **Rouviere-Yaniv, J.** 1978. Localization of the HU protein on the *Escherichia coli* nucleoid. Cold Spring Harbor Symp. Quant. Biol. **42**:439-447.

79. **Rouviere-Yaniv, J., and F. Gros.** 1975. Characterization of a novel, low-molecular weight DNA-binding protein from *Escherichia coli*. Proc. Natl. Acad. Sci. USA. **72**:3428-3432.

80. **Saint Girons, I., I. G. Old, and B. E. Davidson.** 1994. Molecular biology of the *Borrelia*, bacteria with linear replicons. Microbiology. **140**:1803-1816.

81. **Sakaguchi, K.** 1990. Invertrons, a class of structurally and functionally related genetic elements that includes linear DNA plasmids, transposable elements, and genomes of adeno-type viruses. Microbiol. Rev. **54**:66-74.

82. **Salas, M.** 1991. Protein-priming of DNA replication. Annu. Rev. Biochem. **60**:39-71.

83. **Samuels, D. S.** 1995. Electrotransformation of the spirochete *Borrelia burgdorferi*. Methods Mol. Biol. **47**:253-9.

84. **Samuels, D. S., and C. F. Garon.** 1993. Coumermycin A_1 inhibits growth and induces relaxation of supercoiled plasmids in *Borrelia burgdorferi*, the Lyme disease agent. Antimicrob. Agents Chemother. **37**(1):46-50.

85. **Samuels, D. S., K. E. Mach, and C. F. Garon.** 1994. Genetic transformation of the Lyme disease agent *Borrelia burgdorferi* with a coumarin-resistant *gyrB*. J. Bacteriol. **176**:6045-6049.

86. **Samuels, D. S., R. T. Marconi, W. M. Huang, and C. F. Garon.** 1994. *gyrB* mutations in coumermycin A_1-resistant *Borrelia burgdorferi*. J. Bacteriol. **176**:3072-3075.

87. **Shore, D., J. Langowski, and R. L. Baldwin.** 1981. DNA flexibility studied by covalent closure of short fragments into circles. Proc. Natl. Acad. Sci. USA. **78**(8):4833-4837.

88. **Sohaskey, C. D., C. Arnold, and A. G. Barbour.** 1997. Analysis of promoters in *Borrelia burgdorferi* by use of a transiently expressed reporter gene. J. Bacteriol. **179**(21):6837-6842.

89. **Stockley, P. G.** 1994. Filter-binding assays, p. 251-262. *In* G. G. Kneale (ed.), DNA-protein interactions: principles and protocols, vol. 30. Humana Press Inc., Totowa, N.J.

90. **Surette, M. G., and G. Chaconas.** 1989. A protein factor which reduces the negative supercoiling requirement in the Mu DNA strand transfer reaction is *Escherichia coli* integration host factor. J. Biol. Chem. **264**(5):3028-3034.

91. **Suzuki, M., N. Yagi, and J. T. Finch.** 1996. An in-the-groove view of DNA structures in complexes with proteins. J. Mol. Biol. **255:** 677-687.

92. **Svarchevsky, A. N., and V. N. Rybchin.** 1984. Characterization of plasmid properties of bacteriophage N15. Mol. Genet. Mikrobiol. Virusol. **5:**34-39.

93. **Swanberg, S. L., and J. C. Wang.** 1987. Cloning and sequencing of the *Escherichia coli gyrA* gene coding for the A subunit of DNA gyrase. J. Mol. Biol. **197:**729-736.

94. **Tilly, K., S. Casjens, B. Stevenson, J. L. Bono, D. S. Samuels, D. Hogan, and P. Rosa.** 1997. The *Borrelia burgdorferi* circular plasmid cp26: conservation of plasmid structure and targeted inactivation of the *ospC* gene. Mol Microbiol. **25**(2):361-73.

95. **Tilly, K., J. Fuhrman, J. Campbell, and D. S. Samuels.** 1996. Isolation of *Borrelia burgdorferi* genes encoding homologues of DNA-binding protein HU and ribosomal protein S20. Microbiology. **142:**2471-2479.

96. **Tilly, K., L. Lubke, and P. Rosa.** 1998. Characterization of circular plasmid dimers in *Borrelia burgdorferi*. J. Bacteriol. **180**(21):5676-5681.

97. **Travers, A. A., S. S. Nerr, and M. E. A. Churchill.** 1994. DNA chaperones: a solution to a persistence problem? Cell. **77:**167-169.

98. **Varshavsky, A. J., S. A. Nedospasov, V. V. Bakayev, T. G. Bacayeva, and G. Georgiev.** 1977. Histone-like proteins in the purified *Escherichia coli* deoxyribonucleoprotein. Nucleic Acids. Res. **4:**2725-2745.

99. **Wada, M., Y. Kano, and T. Ogawa.** 1988. Construction and characterization of the deletion mutant of *hupA* and *hupB* genes in *Escherichia coli*. J. Mol. Biol. **204:**581-591.

100. **Wang, J. C.** 1996. DNA topoisomerases. Annu. Rev. Biochem. **65:**635-692.

101. **Watson, J. D.** 1972. Origin of concatemeric T7 DNA. Nature New Biol. **239:**197-201.

102. **Watson, M. A., and G. Chaconas.** 1996. Three-site synapsis during Mu DNA transposition: a critical intermediate preceding engagement of the active site. Cell. **85:**435-445.

103. **Wu, F., A. Kolb, and H. Buc.** 1982. A transcriptionally active plasmid-protein complex isolated from *Escherichia coli*. Biophys. Acta. **696:**231-238.

104. **Zhang, J., J. M. Hardham, A. G. Barbour, and S. J. Norris.** 1997. Antigenic variation in Lyme disease borreliae by promiscuous recombination of VMP-like sequence cassettes. Cell. **89:**275-285.

105. **Zuckert, W. R., and J. Meyer.** 1996. Circular and linear plasmids of Lyme disease spirochetes share extensive homology: characterization of a repeated DNA element. J. Bacteriol. **178:**2287-2298.